UNIVERSITÄTSKLINIKUM HAMBURG-EPPENDORF

Institut für Anatomie und Experimentelle Morphologie

Direktor: Prof. Dr. med. Udo Schumacher

Die Bedeutung von Selektinen für das Tumorwachstum und die Metastasierung von humanen Neuroblastomzellen

Dissertation

zur Erlangung des Grades eines Doktors der Medizin
an der Medizinischen Fakultät der Universität Hamburg.

vorgelegt von:

Nina Schwankhaus-Bade
aus Kronberg im Taunus

Hamburg 2014

Angenommen von der
Medizinischen Fakultät der Universität Hamburg am: 23. Februar 2016

Veröffentlicht mit Genehmigung der
Medizinischen Fakultät der Universität Hamburg.

Prüfungsausschuss, der/die Vorsitzende: Prof. Dr. Udo Schumacher

Prüfungsausschuss, zweite/r Gutachter/in: PD Dr. Andreas Block

Prüfungsausschuss, dritte/r Gutachter/in:

Inhaltsverzeichnis

RESEARCH PAPER

Cell adhesion molecules in metastatic neuroblastoma models

Nina Schwankhaus · Christina Gathmann ·
Daniel Wicklein · Kristoffer Riecken ·
Udo Schumacher · Ursula Valentiner

Abstract Several cell adhesion molecules (CAMs) including selectins, integrins, cadherins and immunoglobulin-like CAMs are involved in leukocyte adhesion especially at sites of inflammation. In cancer cells, these CAMs have been associated with the growth and metastatic behavior in several malignant entities. In this study adhesion of LAN 1 and SK-N-SH neuroblastoma cells to selectins, hyaluronan and endothelial cells were determined under flow conditions. Furthermore cells were injected subcutaneously into wildtype and selectin deficient scid mice and their growth and metastatic behavior were analyzed. Under shear stress SK-N-SH cells firmly adhered to E-selectin-Fc-fusion protein, hyaluronan and endothelial cells, while LAN 1 cells showed less or hardly any adhesive events by comparison. In the SK-N-SH xenograft model metastasis formation was slightly dependent on the expression of selectins, while LAN 1 cells developed metastases completely independent of selectin expression. The different adhesive and metastatic properties of LAN 1 and SK-N-SH cells are reflected by a different expression profile of several CAMs. The results indicate that endothelial selectins are not essential for metastasis formation of human LAN 1 and SK-N-SH cells. However, other CAMs namely CD44, N-cadherin, NCAM and integrins were upregulated or downregulated, respectively, in SK-N-SH and LAN 1 cells and are potential adhesion molecules involved in the metastatic cascade of these cells.

Keywords Cell adhesion molecules · Metastasis · Neuroblastoma · Scid mouse · Selectin · Xenograft

Introduction

Neuroblastoma is an embryonic tumor that arises from the sympathetic nervous system and represents the most common solid neoplasm of childhood [1, 2]. Although spontaneous regression can occur in children <1 year old, by the time of diagnosis neuroblastoma has already spread in 70 % of the patients to distant organs [1–3]. Frequent sites for metastases include bone marrow (70.5 %), bone (55.7 %), lymph nodes (30.9 %) and liver (29.6 %) [4]. Once the process of metastasis formation has begun, the outcome of therapy is minimal [1].

Metastasis is a complex multistep process, comprising the separation of tumor cells from a primary tumor and local invasion, the intravasation into the blood or lymphatic circulation, the evasion of host defenses while in the bloodstream, the adhesion to the vascular endothelium at the site of future metastasis in distant organs, and the extravasation and colonization at distant sites [5]. Adhesive properties of cells are mediated by the family of cell adhesion molecules (CAMs) and include selectins, integrins (ITGs), cadherins and immunoglobulin-like CAMs (ICAM-1, VCAM-1, NCAM). Many of these CAMs such as selectins, N-cadherin, ITGs physiologically mediate transient adhesion of leukocytes and platelets to endothelial cells in inflammatory processes [6].

N. Schwankhaus · C. Gathmann · D. Wicklein ·
U. Schumacher · U. Valentiner (✉)
Center for Experimental Medicine, Institute of Anatomy and
Experimental Morphology, University Medical Center
Hamburg-Eppendorf, Martinistr. 52, 20246 Hamburg, Germany
e-mail: valentin@uke.uni-hamburg.de; valentiner@uke.de

K. Riecken
Research Department Cell and Gene Therapy, Clinic for Stem
Cell Transplantation, Center for Oncology, University Medical
Center Hamburg-Eppendorf, Martinistr. 52, 20246 Hamburg,
Germany

Springer

The roles of CAMs during the metastatic cascade are partially opposing. As epithelial cells are tightly bound to each other and to the basement membrane and are not motile, CAMs which mediate cell to cell contacts within the primary tumor have to be downregulated for separation and invasion of tumor cells. It is assumed that migration and invasion of epithelial cancer cells go along with profound phenotypic changes that include the loss of especially homotypic cell–cell adhesion, the loss of cell polarity, and the acquisition of migratory and invasive properties referred to as the epithelial to mesenchymal transition (EMT) [7, 8]. EMT occurs during critical phases of embryonic development such as gastrulation and neural crest formation and is admittedly involved in metastatic events in epithelial cancer [9, 10]. Although neuroblastoma is of neuroectodermal origin, neuroblastoma cells also undergo EMT-like changes when adopting an invasive or metastatic phenotype [11, 12].

In contrast, CAMs which mediate the adhesion to endothelial cells have to be upregulated at the site of extravasation. Heterotypic interactions between circulating tumor cells (CTCs) and endothelial cells are necessary to facilitate tethering and arrest of blood-borne cancer cells to endothelial cells as the initial step in the growth of a metastatic tumor. These interactions are mediated by a variety of CAMs such as the selectin and ITG family, which are also involved in the leukocyte adhesion cascade [13]. Thus, recent studies of tumor cell–endothelial cell interactions have been based on the model of leukocyte extravasation during the inflammatory response [6, 14–18]. Leukocyte extravasation is divided into sequential steps whereby rolling mediated by cytokine activated endothelial selectins is followed by firmer adhesions particularly between ITG subunits and an activated endothelium, and subsequent transendothelial migration (TEM) [5, 18]. In spite of obvious differences between leukocyte and tumor cell extravasation, the CAMs mediating the contact to endothelial cells are potentially the same [19, 20]. Recent studies confirmed that selectins and ITGs play a role in cancer progression of various cancer types, although it is controversial whether selectin-mediated rolling is necessary for TEM of cancer cells [19, 21]. In neuroblastoma P-selectin mediates adhesion of these cells to platelets, but the importance of selectins for the general process of metastasis formation is still unclear [17, 22, 23]. The focus of this study lies on members of the selectin, ITG, cadherin and immunoglobulin-like CAM (ICAM-1, VCAM-1, NCAM) families, because these serve the adhesion of tumor cells and have accordingly been associated with malignant progression in clinical and experimental studies.

The influence of the above-mentioned CAMs on adhesion and metastasis formation of neuroblastoma cells is investigated in vitro and in a xenograft mouse model which has already been used to model the metastatic cascade for in vivo experimentation [24, 25]. SK-N-SH and LAN 1 neuroblastoma cells were chosen because these cells show a different pattern of pulmonary metastases. LAN 1 cells produce micrometastases in the alveolar interstitium whereas SK-N-SH cells produce multi-cellular metastases predominantly located in the intra- and periarterial space of the lung [25]. These results indicate that these neuroblastoma cells use different mechanisms for adhesion and extravasation in the course of metastasis formation.

Materials and methods

Cell lines and cell culture

SK-N-SH and LAN 1 cells were cultured under standard conditions (37 °C, 100 % humidity, 5 % CO_2). RPMI medium (Gibco/Life Technologies, Paisley, Scotland) with 10 % heat inactivated fetal calf serum (FCS, Gibco), 2 mM L-glutamine (Gibco), 100 U/ml penicillin and 100 μg/ml streptomycin (Gibco) was used as nutrient solution.

Human pulmonary microvascular endothelial cells (HPMEC) were obtained from PromoCell (Heidelberg, Germany). For propagation of endothelial cells, endothelial cell growth medium (PromoCell) supplemented with supplement mix (PromoCell), 10 % FCS and 1 % penicillin and streptomycin was used.

All cells were tested to be free of mycoplasma prior to experimentation.

Fluorescence activated cell sorting (FACS)

Neuroblastoma cells were tested for their ability to bind human E- and P-selectin-Fc- chimera (724-ES, 137-PS, R&D Systems, Minneapolis, USA) and to express selectin ligands CA19-9 (abcam, Cambridge, UK) and CD15 s (BD Biosciences, Heidelberg, Germany) by FACS analyses. Isotype controls for each antibody and Fc-control (R&D Systems) for selectin chimera served as negative controls, respectively. All antibodies were diluted in FACS buffer in a concentration of 2 μg/ml. The respective secondary antibodies (BD Biosciences) were diluted 1:100 in FACS buffer. For production of selectin complexes, 1 μl E-selectin-, P-selectin-Fc-chimera or Fc-control (1 mg/ml), respectively, were prepared with 100 μl FACS-buffer + 1 mM Ca^{2+} + 1 mM Mg^{2+} and complexed by incubation with 1.25 μl goat anti-human-IgG-PE (0.5 mg/ml). Cells were incubated with antibodies or selectin complex, respectively, for 30 min on ice, washed and analyzed using a FACS-Calibur (BD Biosciences). Dead cells and debris were eliminated from analysis on the basis of forward and

sideward light scatter and propidium iodide (Sigma–Aldrich, Hamburg, Germany) staining.

Laminar flow adhesion assay

Laminar flow experiments were performed using IBIDI microslides VI (IBIDI, Munich, Germany) connected to a syringe pump (Model 100 Series; kdScientific, Holliston, Massachusetts, USA) and cell movement was observed with an inverted microscope (Zeiss, Jena, Germany; Axiovert 200). Microslides were coated over night at 37 °C and 5 % CO_2 with recombinant human (rh) 5 µg/ml E- or 50 µg/ml P-selectin-Fc-chimeras (R&D Systems), respectively. Control channels were coated with rh IgG1-Fc (R&D Systems).

Capillaries were covered with human pulmonary microvascular endothelial cells (HPMECs, 30,000 cells per capillary) and incubated until confluence for 24 h. HPMECs were stimulated with 10 ng/ml TNF-α (Pepro-Tech, Hamburg, Germany, Cat.: 300-01A) 4 h prior to each experiment. Non-stimulated HPMECs served as negative controls. Stimulated HPMECs knowing to express E-selectin [26] were incubated with an adhesion blocking E-selectin mAb (BioLegend, San Diego, CA) for 30 min prior to the experiment.

Furthermore slides were coated with hyaluronan (1 mg/ml) and with 1 % BSA as control. Cells were additionally incubated with a hyaluronan blocking CD44 antibody (10 µg/ml; BioLegend) for 30 min at 37 °C and 5 % CO_2 prior to the flow assay.

Neuroblastoma cells were detached with cell dissociation buffer, resuspended in cell culture medium (20 ml, 100,000 cells/ml) and a syringe with the cell suspension was connected to a pump (kdScientific, Holliston, MA, USA, Model 100 Series). Applied shear rates varied from 0.5 to 2.0 dyn/cm^2. Cell movement was recorded and analyzed with regard to cell adhesion using CapImage 8.5 program (Dr. Heinrich Zeintl, Heidelberg, Germany).

Xenograft mouse model

Experiments were conducted using ten severe combined immunodeficient (scid) and ten E- and P-selectin knockout scid mice per cell line from the stock of the University Hospital Hamburg-Eppendorf, Germany. At the beginning of the experiment, average mouse age was 15 weeks and their average weight was 25 g. All animal experiments were approved by the local animal care committee and assigned the project No. 09/88.

The mice were kept in individually ventilated cages, provided with sterile water and food ad libitum. Before being inoculated, 1×10^6 cells were suspended in 100 µl cell culture medium and were blended 1:1 with Matrigel (BD Bioscience, Bedford, USA) to support growth. The mice bearing neuroblastomas were sacrificed when the tumor had reached maximal growth (up to 10 % of the body weight of the animal at the beginning of the experiment) or started to ulcerate. Mice were anesthetized using ketamine/rompun (0.1 ml per 10 g body weight) and blood was extracted from mouse hearts. Dispatching was done by cervical dislocation. Post mortem primary tumor, lung and bone marrow were removed for further examinations.

Histology

Primary tumors and lungs were embedded in paraffin wax and cut into 4 µm thick sections and afterwards stained with hematoxylin-eosin (HE). Primary tumor and lung sections were also used for immunohistochemistry.

The number of pulmonary metastases was determined by examining ten sections from the middle of each block. Pulmonary metastases were counted (magnification 100×) and the mean value of the ten middle sections was multiplied by the number of sections and the factor 0.8 in order to roughly estimate the total number of metastases [27].

Analysis of circulating and disseminated tumor cells

Human tumor cells in blood (CTCs) and in bone marrow (DTCs) were quantified by real-time polymerase chain reaction (PCR) using established primers specific for repetitive, non-coding human Alu sequences as previously described [28, 29]. The experiment was realized with the LightCycler 480 2.0 (Roche diagnostics GmbH, Mannheim, Germany). Bone marrow of the left femur was centrifuged and resuspended in 200 µl PBS. This cell suspension and 200 µl blood were taken for DNA extraction with the QiAamp DNA blood miniKit 250 (Qiagen, Hilden, Germany). For each bone marrow- and blood-sample a 8 µl master mix was established, containing 100 pmol alu forward (TGG CTC ACG CCT GTA ATC CCA) and 100 pmol alu reverse (GCC ACT ACG CCC GGC TAA TTT) as well as LightCycler Mastermix (LightCycler Fast Start DNA Master PLUS SYBR Green I Cat.No. 03515885001, Roche). The PCR conditions were initially 10 min 95 °C, followed by 50 cycles of 5 s 95 °C, 5 s 67 °C and 20 s 72 °C (measurement of fluorescence). Melting curve analysis (0 s 5 °C, 2 s 65 °C and 0 s 95 °C) was performed directly after PCR run. Quantification of CTCs in mouse blood and DTCs in bone marrow was based on standard curves using DNA extracted from blood and bone marrow, respectively, of control mice spiked with DNA isolated from SK-N-SH or LAN 1 neuroblastoma cells grown in culture (1 cell/ml up to 1×10^6 cells/ml).

Table 1 Results of qRT-PCR analysis

	AVG ΔCt (Ct(GOI) − Ave Ct (HKG)) LAN 1	AVG ΔCt (Ct(GOI) − Ave Ct (HKG)) SK-N-SH	Fold up- or down-regulation
CD44	14.67	2.09	−6,122.90 ns
ITGA5	14.77	6.55	−298.17*
ITGB1	3.45	2.18	−2.41*
ICAM-1	14.06	8.79	−38.68*
NCAM	3.12	14.49	2,634.54*
VCAM-1	3.98	14.49	1,454.86 ns

CD44, ITGA5, ITGB1 and ICAM-1 are upregulated, NCAM and VCAM-1 are downregulated in SK-N-SH cells compared with LAN 1 cells

ns not significant

* $p < 0.05$

Quantitative real-time PCR array

The human ECM and cell adhesion RT^2 Profiler PCR Array (SABiosciences) was used for real time PCR array analyses of cDNA processed with RT^2 First strand kit C-03 from RNA extracted from cell culture with RNeasy Mini Handbook Qiagen (Qiagen, Hilden, Germany). The batch for elimination of genome DNA contained 1 μg RNA, 2 μl GE buffer (5× gDNA Elimination Buffer) and 10 μl H_2O. The RT cocktail contained 4 μl BC3 (5× RT Buffer 3), 1 μl P2 (Primer and External Control Mix), 2 μl RE3 (RT Enzyme Mix 3) and 3 μl H_2O. 10 μl of both RT cocktail and genome DNA elimination were mixed and prepared for application on PCR array (PAHS-013F, RT^2 Profiler TM PCR Array human extracellular matrix and adhesion molecules, Lot. DC01, SABiosciences). Five housekeeping genes and internal controls for genomic.

DNA contamination, RNA quality, and general PCR performance were also included. The array was repeated thrice with independently isolated RNA to generate statistically relevant data. ECM and cell adhesion array data were analyzed based on the ΔCt method using an Excel-based data analysis template (SA Bioscience) and were presented as x-fold up- or downregulation (Table 1).

FACS analysis

Expression of CAMs CD44 (Diaclone, Besancon, France), ICAM-1 (Sigma-Aldrich), NCAM (R&D Systems), VCAM-1 (Santa Cruz, Heidelberg, Germany), ITGA5 (eBioscience, San Diego, USA) and ITGB1 (Santa Cruz) was analyzed by FACS. Isotype controls for each antibody served as negative controls. Analyses were performed as described above.

Immunohistochemistry

Monoclonal antibodies were used against the following human antigens: N-cadherin (1:10000; DAKO, Glostrup, Denmark), ICAM-1 (1:500; Sigma-Aldrich), NCAM (1:500; Leica Novocastra, Wetzlar, Germany), VCAM-1 (1:3,000, Santa Cruz), CD44 (1:5,000; BD Pharmingen), ITGA5 (1:250; abcam) and ITGB1 (1:50; Santa Cruz) antibodies. Isotype controls for each antibody served as negative controls. Briefly, sections were dewaxed and pretreated with protease XXIV (0.08 g/200 ml; ITGB1) or with trypsin (0.1 %; N-cadherin) in TBS for 10 min at 37 °C, with a microwave oven in DAKO retrieval solution S1699 (DAKO; ICAM-1 and NCAM) and with steamer in DAKO retrieval solution S1699 or S2367 (DAKO; CD44, ITGA5 or VCAM-1), respectively. Non-specific binding was blocked by incubating the sections in 10 % normal rabbit serum (DAKO) for 30 min at room temperature. Sections were incubated 1 h at 37 °C or overnight at 4 °C with primary antibody, rinsed and then incubated for 30 min at room temperature with the respective secondary biotinylated antibody. Immunohistochemical detection of CD44, N-cadherin, NCAM and VCAM-1 antibodies was performed by using the catalyzed signal amplification system (CSA, Dako), according to the manufacturer's instructions. All other antibodies were detected by the streptavidin–alkaline phosphate kit (ABC-AP; Vector Laboratories). Enzyme reactivity of the alkaline phosphate complex was visualized using DAKO liquid permanent red (DAKO).

Immunohistochemistry was evaluated using a modified immunoreactive score (IRS) [30]. IRS is the product of intensitiy of immunostaining (none = 0; weak = 1; moderate = 2; strong = 3) and the percentage of positive tumor cells <5 % = 0; 5–20 % = 1; 20–50 % = 2; 50–80 % = 3; >80 % = 4). Value of 0 was scored as no expression, values of 1–4 as weak, 5–8 as moderate and 9-12 as strong expression.

shRNA directed against ITGA5, transfection and selection

DNA oligonucleotides targeting human ITGA5 (CAG-CTACCTAGGATACTCT) were ligated into the pLVX-shRNA1 vector (Clontech, Saint-Germain-en-Laye, France) according to the manufacturer's instructions. The anti-ITGA5 sequence was checked for potential off-target effects using PubMed BLAST. The same vector containing shRNA against firefly luciferase was used to generate control cells (shLuc). Viral particles were produced as cell-free supernatants by transient transfection of HEK-293T packaging cells as described [31, 32]. In brief, lentiviral vectors based on pLVX-shRNA1 were packaged using the second-generation

packaging plasmid psPAX2 (Addgene #12260) and phCMV-VSV-G [33] expressing the envelope protein of vesicular stomatitis virus. The supernatant was harvested 24 h after transfection, 0.45 μm filtered and stored at -80 °C. Target cells were plated at 5×10^4 cells in 0.5 ml medium in each well of a 24 well plate. After addition of viral particle containing supernatant to the cells, the medium was replaced the next day and puromycin was added the second day after transduction at a concentration of 1 μg/ml. The puromycin selection was carried out for at least 1 week. SK-N-SH cells transduced with ITGA5 shRNA were sorted after staining with ITGA5-FITC antibody using the FACSAria cell sorter (BD, Heidelberg, Germany). All stably transfected SK-N-SH cells were analysed with regard to ITGA5 silencing. After cell sorting SK-N-SH shITGA5 cells were expanded and pooled. RNA interference efficiency was verified by flow cytometry. SK-N-SH shLuc cells served as control cells.

Cell migration assay

The migration assay was performed with the 24-well plate FluoroBlok system from BD Biosciences with a pore size of 8 μm. For migration assay cells were washed with phosphate buffered saline solution (PBS) (GIBCO) and resuspended in RPMI medium without FCS. The inserts were filled with 400 μl cell suspension (300,000 cells/ml), and the bottom chambers were filled with 1,200 μl RPMI with 10 % FCS. The cells were allowed to migrate through insert filters for 24 h at 37 °C in a 5 % CO_2 incubator. The migrated cells were quantified by labeling with the Calcein acetoxymethylester (Calcein AM) fluorescent dye (4 μg/ml in HBSS, 1 h incubation), and measuring the fluorescent signal by a bottom plate reader Tecan Spectrafluor (Tecan Group Ltd., Männedorf, Schweiz). Experiments were performed in triplicate and repeated two times.

Leukocyte detection and counting in lungs by CD45 immunohistochemistry

Leukocytes in the lungs were stained by CD45 immunohistochemistry (1:25; BD Pharmingen). Lung sections were pretreated with microwave in DAKO retrieval solution S1699 and subsequent immunohistochemistry was performed as described above. For quantitative assessment of leukocytes, CD45 positive cells were counted in two representative sections of each lung in ten randomized different microscopic fields, respectively.

Statistical analysis

Results of laminar flow assay and migration assay were compared with an analysis of variance (one-way ANOVA) and Bonferroni's post test and with two-tailed Student's

t test, respectively. The statistical analyses of the xenograft model and leukocyte cell counting were performed using a two-tailed Student's t test for t distributed random variables. As numbers of pulmonary metastases, CTCs in blood and DTCs in bone marrow, respectively, showed log-normal distribution, values were log-transformed before statistical analysis. Two-tailed Student's t test was used to compare values of scid and scid select mouse groups. Numbers of lung metastases and DTCs were also evaluated by an analysis of covariance (ANCOVA) with factor primary tumor weight and factor CTCs in blood, respectively, and including interaction terms of mouse group*primary tumor weight and mouse group*CTCs in blood, respectively. These non-significant interactions were omitted (backwards selection) and the effect estimated of the final model was presented with p value. These statistical tests were carried out using IBM SPSS statistics software (SPSS version 18.0 for Windows, IBM, Ehningen, Germany). $p < 0.05$ was considered as a statistically significant result. All data were visualized using Graph Pad Prism 5.0 (GraphPad Software, San Diego, California, USA).

Results

Binding and adhesion of neuroblastoma cells in vitro

The binding of human E- and P-selectin-Fc-fusion proteins and expression of selectin ligands CA19-9 and CD15s were examined by FACS analyses (Fig. 1). SK-N-SH cells bound to P-selectin-Fc-fusion protein and to a lesser extent to anti-CA19-9 and anti-CD15 s antibodies, while there is only a small amount of E-selectin-Fc-fusion protein binding. LAN 1 cells showed moderate P-selectin-Fc-fusion protein binding, but only single cells bound to E-selectin-Fc-fusion protein and were positive for CD15s and CA19-9.

In laminar flow assay SK-N-SH and LAN 1 cells adhered to E-selectin-Fc-fusion protein (Fig. 2a, b). SK-N-SH cells showed a higher number of cells adhering to E-selectin-Fc-fusion protein than LAN 1, especially at 50 μg/ml with a shear stress of 0.5 dyn/cm^2 (16 vs. 4 adhesive events, $p < 0.05$). Remarkably, cells which finally adhered, showed strong affinity to E-selectin-Fc-fusion protein and could not be released from the capillary surface even after application of high shear stress.

Neuroblastoma cell movement on rh P-selectin-Fc-chimera coated surface differed from that on E-selectin-Fc-fusion protein. On microslides coated with 50 μg/ml P-selectin-Fc-fusion protein, there was only very few adhesion to be seen at a shear stress of 0.5 dyn/cm^2 in both cell lines. Instead, tethering, an alternating cell adhesion and release could be observed at a shear stress of 0.5 dyn/cm^2 (data not shown). At higher shear
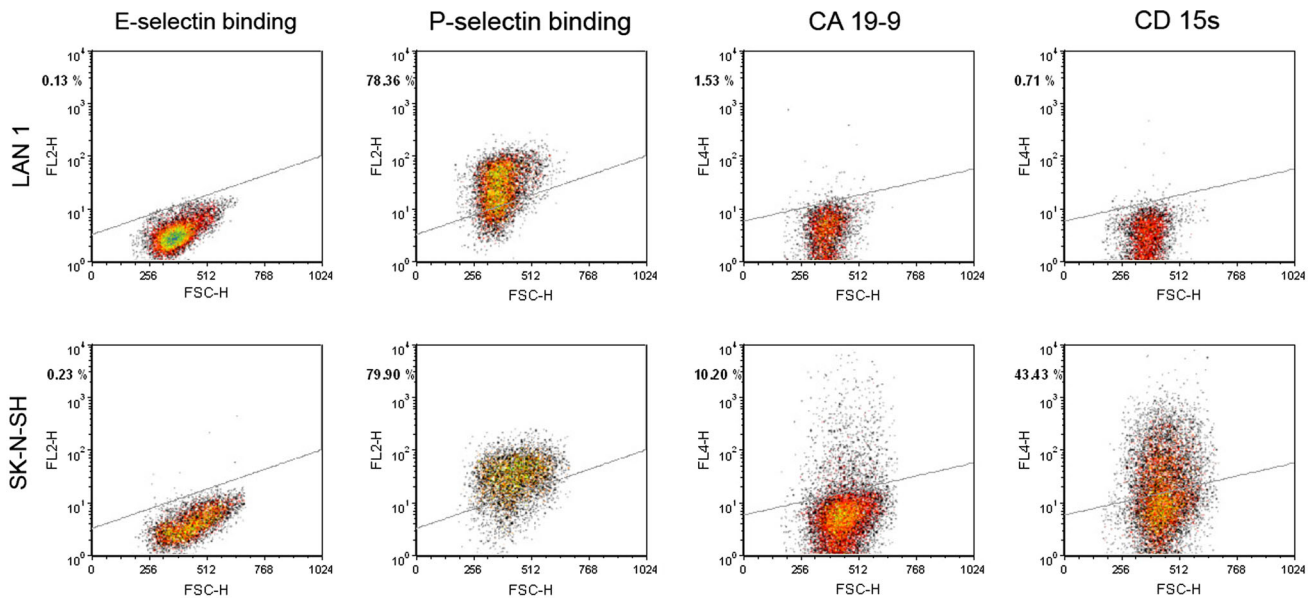
Fig. 1 E- and P-selectin-Fc-fusion proteins binding sites, CD15s and CA19-9 expression on SK-N-SH and LAN 1 neuroblastoma cells. Cells showed P-, but rarely E-selectin-Fc-fusion protein binding. In contrast to LAN 1 cells, SK-N-SH cells express CD15s and CA19-9, which are known E-selectin ligands. Thus, SK-N-SH cells can bind to E-selectin via these ligands in principle

stress P-selectin-Fc-fusion protein could not mediate any cell adhesion or tethering.

SK-N-SH cells showed more adhesive events to TNF-α stimulated than to unstimulated HPMECs (3 vs. 17 adhesive events, $p < 0.01$). Incubation with an adhesion blocking anti-E-selectin (CD62E) mAb reduced SK-N-SH cell adhesion to 50 % ($p < 0.05$). LAN 1 cells showed rarely adhesion to unstimulated and stimulated HPMECs under shear stress (0 and 3 adhesive events, respectively) (Fig. 2c). Application of high shear stress released tumor cells from the HPMECs indicating only moderate binding strengths.

Whereas CD44 positive SK-N-SH cells showed about 20 adhesive events to hyaluronan at all tested shear stresses, CD44 negative LAN 1 cells did not stick to hyaluronan coated slides. Adhesion of SK-N-SH cells to hyaluronan was significantly blocked by an anti-CD44 antibody ($p < 0.01$; Fig. 2d).

Xenograft mouse model

Results of the animal experiment are demonstrated in Fig. 3. All inoculated mice developed primary tumors. Primary tumor weights and tumor growth showed no significant difference between scid and scid select mice. Mean tumor weight in the SK-N-SH group was 1.18 g for both mouse groups. Average tumor growth amounts to 36 and 37 days in SK-N-SH scid and scid select mice, respectively. All SK-N-SH scid mice ($n = 10$) and seven of ten SK-N-SH scid select mice developed lung metastases. SK-N-SH pulmonary metastases were predominantly located in the intra- and periarterial space of the lung and ranged from 144 to 1,795 (mean: 546) in scid and from 0 to 1,240 (mean: 335) in scid select mice (Fig. 3). In scid wildtype mice inoculated with SK-N-SH cells, lung metastases were increased by factor 7.2 compared with scid select mice ($p = 0.052$). Including primary tumor weight as covariate (ANCOVA) number of lung metastases in SK-N-SH was significantly higher in scid than in scid select mice by factor 6.8 ($p < 0.05$; Fig. 3). Number of CTCs in blood and DTCs in bone marrow did not show significant differences between scid and scid select mice within the SK-N-SH group.

In the LAN 1 group the average tumor weight was 1.98 g for scid mice and 2.06 g for scid select mice. In LAN 1 scid mice tumor growth averaged 40 days, and in LAN 1 scid select mice 32 days. Seven of ten scid mice and all scid select mice ($n = 10$) inoculated with LAN 1 cells produced pulmonary micrometastases located in the alveolar septae. Number of metastases varied from 0 to 11,543 (mean: 4,135) in LAN 1 scid and from 594 to 8,624 (mean: 2,770) in scid select mice. In t test analysis and ANCOVA the number of pulmonary metastases in LAN 1 was not significantly different between scid and scid select mice. Numbers of CTCs in blood and DTCs in bone marrow were significantly higher in scid select (mean: 64,511) than in scid mice (mean: 43,898) within the LAN 1 group (Fig. 3). LAN 1 CTCs were increased by factor 7.0 in scid select mice in the LAN 1 group compared with scid mice ($p < 0.05$). Mean of DTCs in bone marrow was
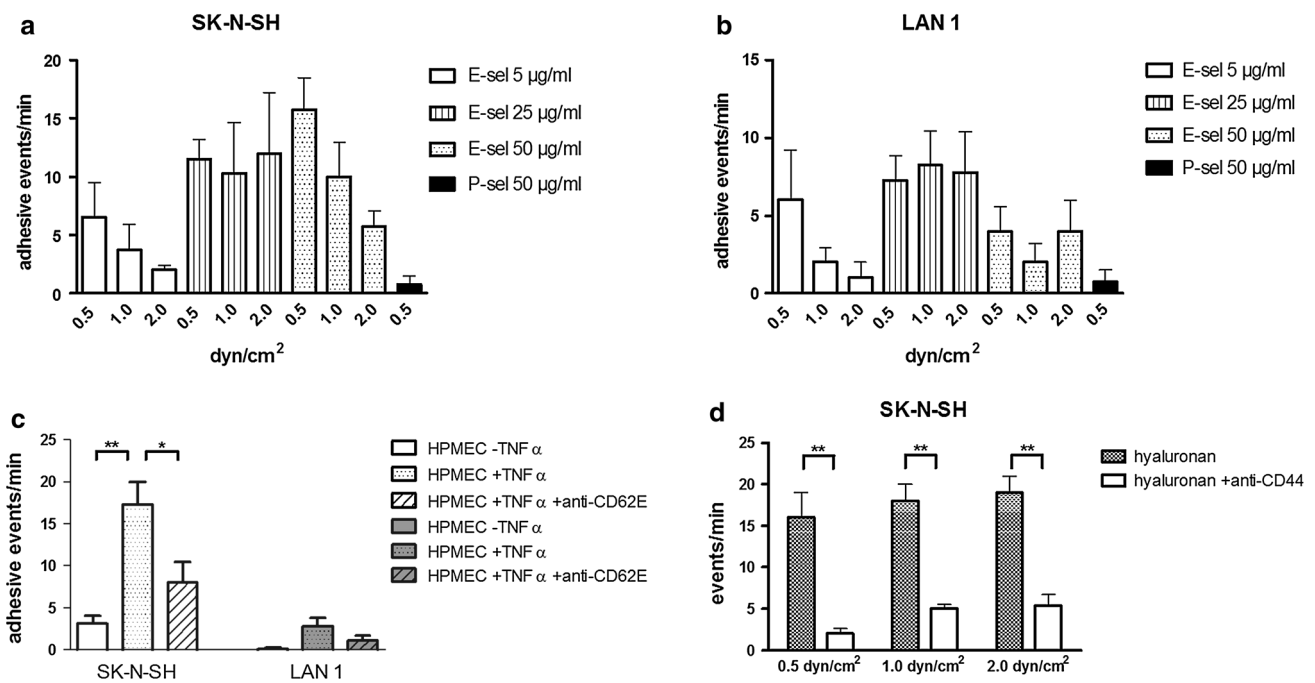
Fig. 2 Cell flow analysis of human neuroblastoma SK-N-SH and LAN 1 cells on rh E- and P-selectin-Fc-chimera at different concentrations and shear stresses (**a**, **b**), on confluent monolayers of TNF-α stimulated and unstimulated human pulmonary microvascular endothelial cells (**c**) and on HA coated capillaries (**d**). **a**, **b** SK-N-SH cells showed a higher number of cells adhering to E-selectin-Fc-fusion protein than LAN 1, especially at 50 μg/ml with a shear stress of 0.5 dyn/cm². Only very few adhesive events can be detected on rh P-selectin-Fc-chimera-coated microslides (50 μg/ml) in both cell lines. **c** SK-N-SH cells showed more adhesive events to TNF-α stimulated than to unstimulated HPMECs (3 vs. 17 adhesive events,

$p < 0.01$) at a shear stress of 0.5 dyn/cm². Incubation with an adhesion blocking anti-E-selectin mAb reduced SK-N-SH cell adhesion to 50 % ($p < 0.05$). LAN 1 cells rarely showed adhesion to unstimulated and stimulated HPMECs under shear stress (0 and 3 adhesive events, respectively). **d** Number of cell flow events of SK-N-SH on HA coated capillaries with and without pre-incubation with HA-blocking CD44 antibody at different shear stresses. The number of total events decreases significantly after incubation with the HA-blocking CD44 antibody. CD44 negative LAN 1 cells did not adhere at all to HA coated slides. *$p < 0.05$, **$p < 0.01$

189 cells/ml in LAN 1 scid group and 417 cells/ml in scid select group (Fig. 3). *T* test analysis showed an increase by factor 3.9 in LAN 1 scid select mice over scid mice ($p < 0.01$).

Comparing LAN 1 and SK-N-SH scid mice, number of CTCs in blood and of lung metastases, respectively, were significantly lower in SK-N-SH scid mice (mean: CTCs 146 cells/ml, lung metastases 546) than in LAN 1 scid mice (mean: CTCs 43,898 cells/ml, lung metastases 4,135; $p < 0.001$ and $p < 0.01$, respectively).

Quantitative real-time PCR array

The quantity of mRNA determined by a real-time PCR array showed a higher expression of ITGA5 ($p < 0.05$), ITGB1 ($p < 0.05$), ICAM-1 ($p < 0.05$) and CD44 (not significant) mRNA in SK-N-SH cells than in LAN 1 cells. LAN 1 cells, however, upregulated NCAM 1 ($p < 0.05$) and VCAM-1 (not significant) mRNA in comparison to SK-N-SH cells (Table 1).

FACS and immunohistochemical analyses

The results of the FACS analyses are presented in Fig. 4. NCAM and ITGB1 could be found on the surface of LAN 1 cells, but not CD44, ICAM-1, VCAM-1 and ITGA55. Corresponding to the PCR array data, SK-N-SH cells were positive for CD44, ICAM-1, ITGA5 and ITGB1 in FACS analyses, but did not express NCAM and VCAM-1.

The results of the immunohistochemical analyses are summarized in Table 2 and Figs. 5, 6, 7. Immunohistochemical staining of primary tumors and lungs exhibited no differences between scid and scid select mouse groups within one cell line and predominantly corresponded to the FACS results except for ICAM-1 and ITGA5.

In summary, SK-N-SH cells exhibited a higher expression of CD44, ITGA5 and B1 than LAN 1 cells in immunohistochemistry. However, SK-N-SH cells were negative for NCAM, which was strongly expressed by LAN 1 cells. N-cadherin was expressed in both neuroblastoma cell lines without differences

Fig. 3 Primary tumor weight, tumor growth, number of lung metastases, CTCs in blood and DTCs in bone marrow of scid and scid select mice in LAN 1 and SK-N-SH group. Data are presented as mean ± SEM. As values of number of lung metastases, CTCs in blood and DTCs in bone marrow have log-normal distributions, these data were log-transformed before statistical analyses. *T* test analyses of primary tumor weight, tumor growth and number of lung metastases did not show a significant difference between scid and scid select mice in LAN 1 and SK-N-SH mice. However, lung metastases were significantly reduced in scid select mice compared with scid mice in SK-N-SH group under consideration of primary tumor weight (ANCOVA, $p < 0.05$). Covariate was fixed at the following value: tumor weight = 1.18 g. Numbers of CTCs in blood and of DTCs in bone marrow were significantly higher in scid select than in scid mice inoculated with LAN 1. In SK-N-SH no significant differences in CTCs in blood and DTCs in bone marrow between wildtype and selectin deficient scid mice can be detected. *$p < 0.05$, **$p < 0.01$
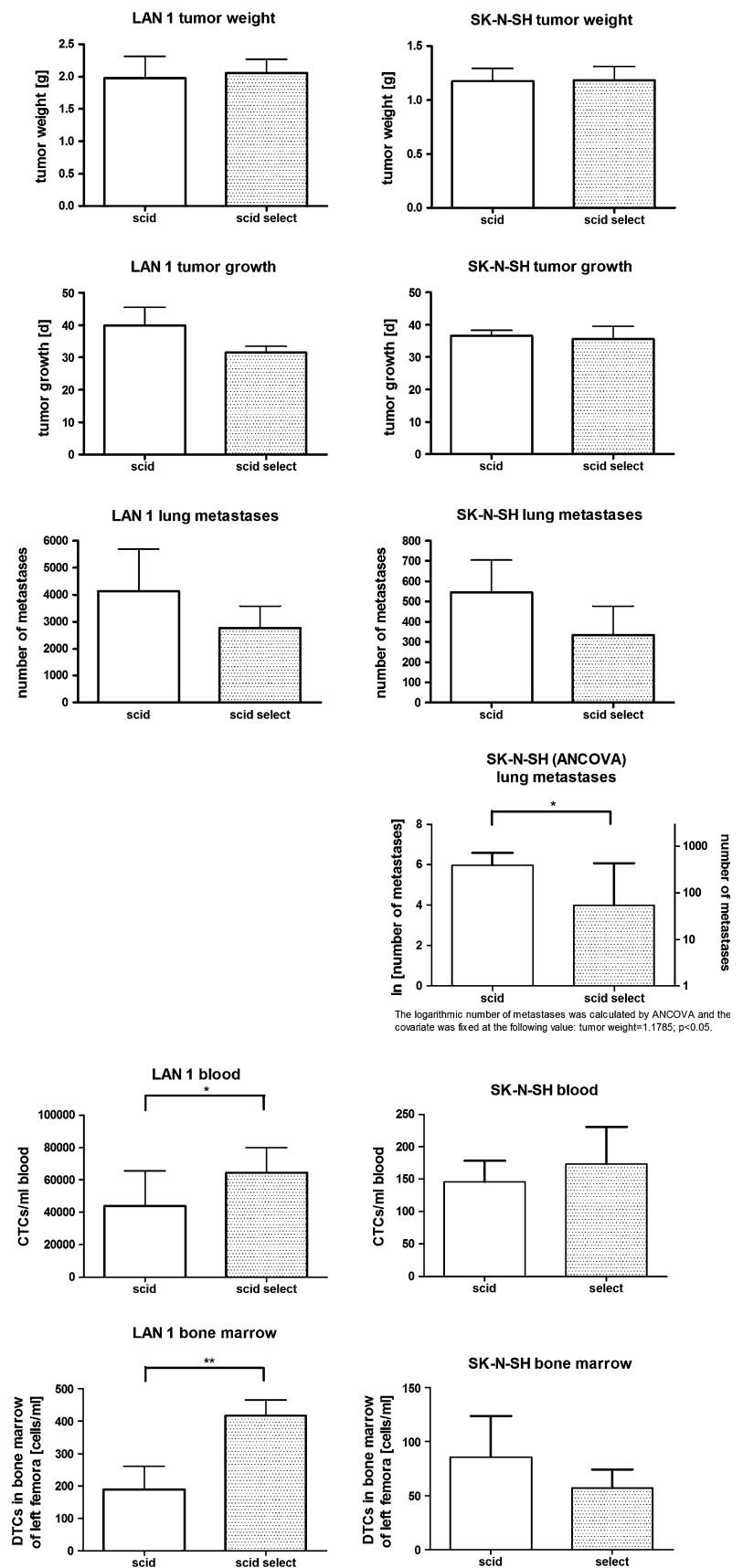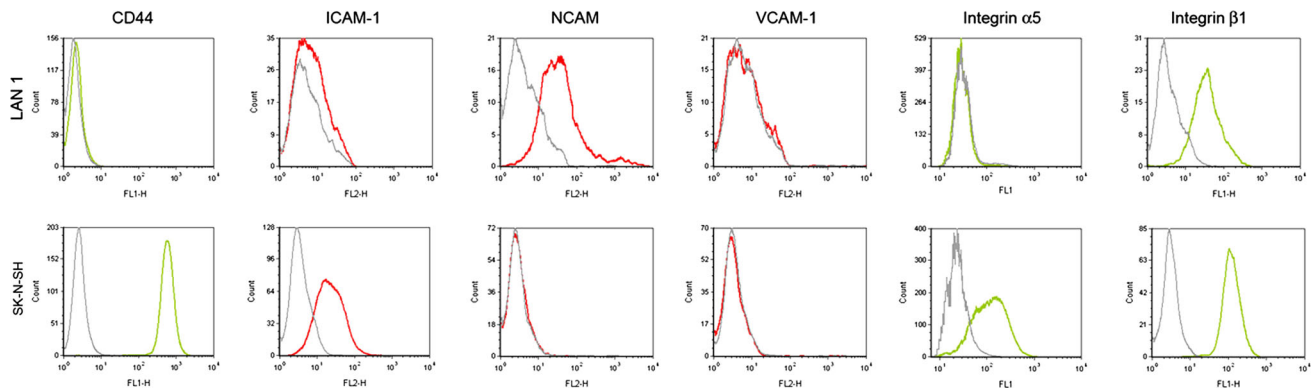
Fig. 4 Cell flow cytometry diagrams showing CD44, ICAM-1, NCAM, VCAM-1, ITGA5 and ITGB1 expression on LAN 1 and SK-N-SH neuroblastoma cell surfaces. The *grey peaks* represent the background profile of cells stained with the isotype control. In FACS analyses LAN 1 cells express NCAM and ITGB1, SK-N-SH cells express CD44, ICAM-1, ITGA5 and ITGB1

Table 2 Immunohistochemical staining of human neuroblastoma LAN 1 and SK-N-SH cells

	LAN 1			SK-N-SH		
	Cells grown in culture	primary tumor	lung metastasis	Cells grown in culture	Primary tumor	Lung metastasis
CD44	−	−	−	+++	++ to +++	+++
ITGA5	+	+	+ to ++	+++	+++	+++
ITGB1	++	+	++ to +++	++ to +++	++	+++
ICAM-1	−	−	−	−	−	−
NCAM	+++	++ to +++	+++	−	−	−
VCAM-1	−	−	−	−	−	−
N-cadherin	+++	+ to ++	+++	+++	+ to ++	+++

The intensity of binding was assessed semi-quantitatively [30]. Staining intensity is classified into negative (−), weak (+), moderate (++) and strong (+++). SK-N-SH cells exhibited a higher expression of ITGA5, ITGB1 and CD44 than LAN 1 cells, but they did not express NCAM, which was strongly expressed by LAN 1 cells

in staining intensity. All neuroblastoma cells were negative for ICAM-1 and VCAM-1 in immunohistochemistry. Staining intensity with anti-N-cadherin and anti-ITGB1 was lower in primary tumors than in cells grown in vitro and embedded in paraffin, and lung metastases for both cell lines.

shRNA directed against ITGA5, transfection and selection

Four selected single cell clones of SK-N-SH shITGA5 were pooled and expanded for further experiments. ITGA5 downregulation of pooled SK-N-SH shITGA5 cells was about 75 % compared to SK-N-SH shLuc control cells.

Cell migration assay

In vitro migratory potential of LAN 1 and SK-N-SH cells was significantly different (Fig. 8). Migration of ITGA5 negative LAN 1 cells was significantly lower compared to ITGA5 positive SK-N-SH shLuc cells ($p < 0.01$). However, silencing of ITGA5 by RNAi increased cell migration of SK-N-SH cells significantly ($p < 0.05$).

Leukocyte detection and counting in lungs by CD45 immunohistochemistry

Leukocytes were irregularly distributed in the lungs showing few areas with up to 30 leukocytes and most fields of views without or with single leukocytes only. Comparison of means between scid (LAN 1:0.7 cells/microscopic field, SK-N-SH 1.7 cells/microscopic field) and scid select mice (LAN 1: 1.5 cells/microscopic field, SK-N-SH: 1.9 cells/microscopic field) presented no significant difference in number of leukocytes in the interstitial tissue of the lung.
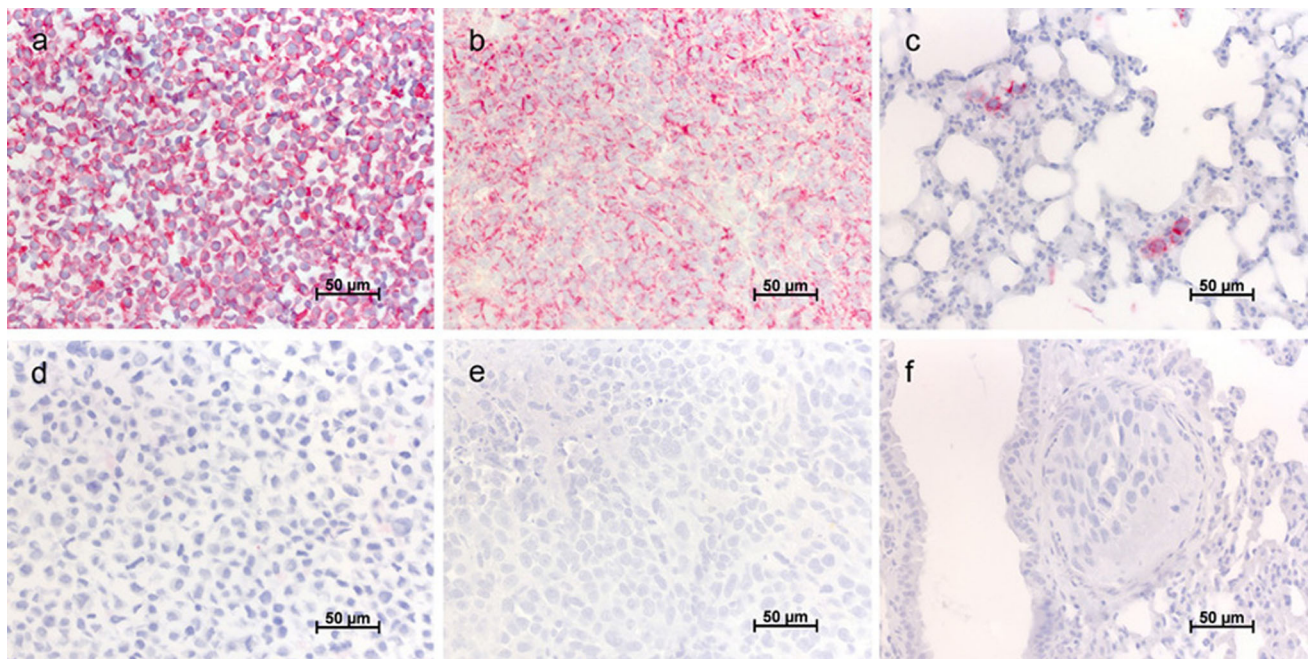
Fig. 5 Representative photomicrographs of NCAM expression of LAN 1 (**a–c**) and SK-N-SH (**d–f**) cells grown in culture (**a**, **d**), primary tumors (**b**, **e**) and lung metastases (**c**, **f**). LAN 1 cells strongly express NCAM, SK-N-SH cells are NCAM negative
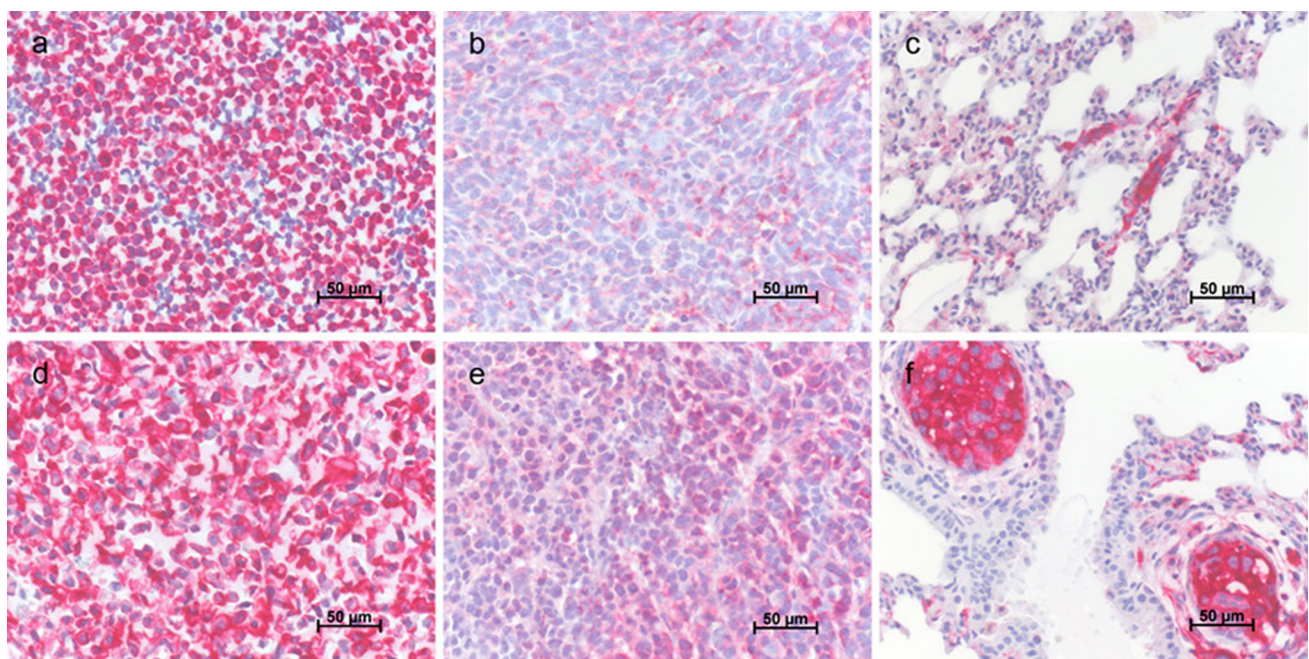

Fig. 6 Representative photomicrographs of ITGA5 expression of LAN 1 (**a–c**) and SK-N-SH (**d–f**) cells grown in culture (**a**, **d**), primary tumors (**b**, **e**) and lung metastases (**c**, **f**). SK-N-SH cells reacted considerably with anti-ITGA5 antibody, whereas LAN 1 cells showed weak immunoreactivity

Discussion

The present study was performed to examine the role of selectins and other CAMs in metastasis formation of neuroblastoma. Selectins are cell-surface carbohydrate-binding proteins expressed on blood platelets (P-selectin) and on endothelial cells (E-selectin) that have been activated by an inflammatory response and mainly mediate
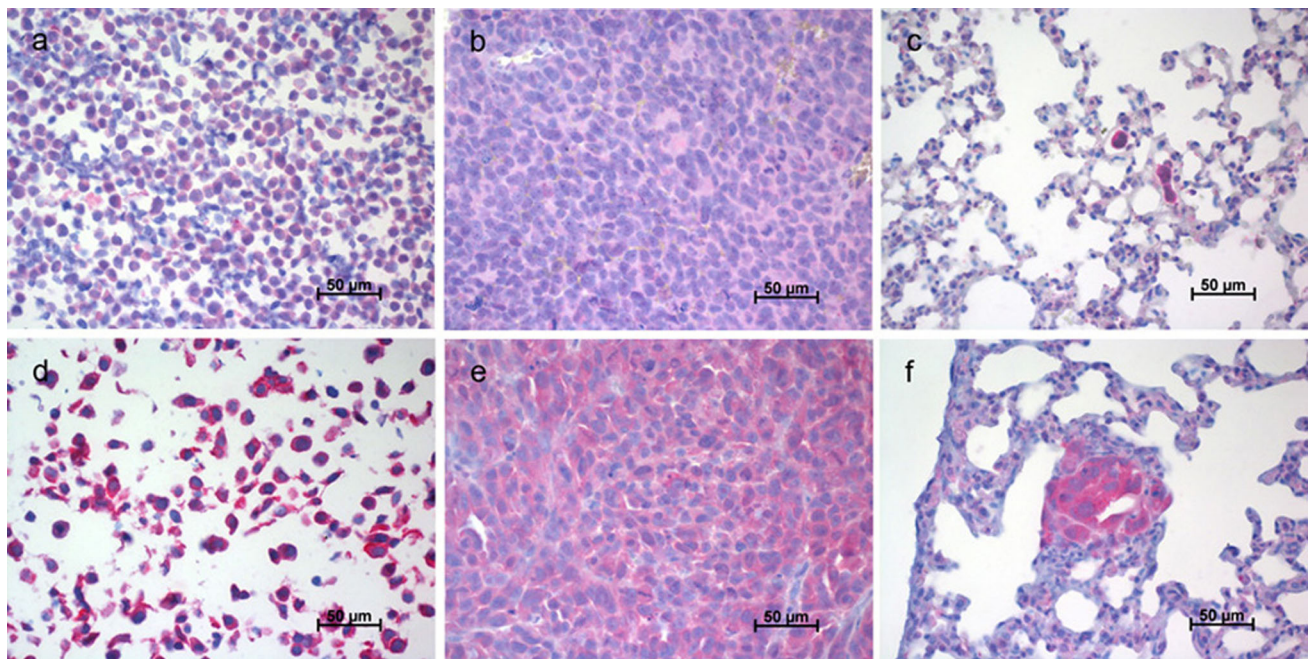
Fig. 7 Representative photomicrographs of ITGB1 expression of LAN 1 (**a–c**) and SK-N-SH (**d–f**) cells grown in culture (**a, d**), primary tumors (**b, e**) and lung metastases (**c, f**). SK-N-SH showed stronger immunoractivity with anti-ITGB1 than LAN 1 cells
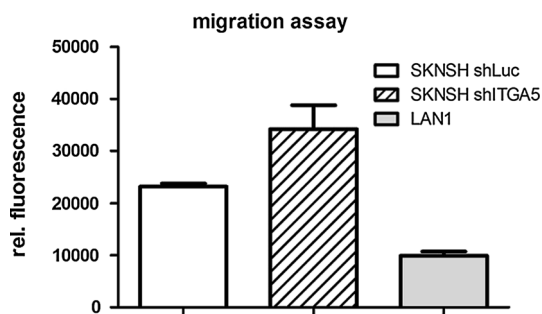

Fig. 8 Fluoroblok migration assay of neuroblastoma cells. Silencing of ITGA5 in SK-N-SH cells increased cell migration. LAN 1 cells showed lowest migratory potential in vitro

rolling of leukocytes on endothelial cells [18, 34]. Selectin-mediated adhesion of cancer cells to vascular endothelium is thought to be closely associated with hematogenous metastasis of cancer [19, 35, 36]. This crucial importance for hematogenous metastasis has been confirmed for breast cancer, pancreatic adenocarcinoma and colon carcinoma in recent studies [37–40]. Results of our in vitro investigations indicate that the influence of selectins on neuroblastoma—endothelial cell adhesion is different between the two cell lines. In the laminar flow assay, LAN 1 cells rarely adhered to recombinant E-selectin-Fc-fusion protein (4 events) and TNF-α stimulated HPMECs (3 events), while SK-N-SH cells showed more adhesive events to recombinant E-selectin-Fc-fusion protein (16 events) and to

stimulated HPMECs (17 events). Binding of SK-N-SH cells to stimulated HPMECs is inhibited by an anti-E-selectin antibody (8 events) confirming that these cells can interact with E-selectin. In FACS analyses, canonical E-selectin ligands CA19-9 and CD15 s are weakly expressed by SK-N-SH and hardly so by LAN 1 cells. Both SK-N-SH and LAN 1 cells bound rarely to E-selectin-Fc-fusion protein in FACS analyses, but to P-selectin-Fc-fusion protein. Under shear stress both neuroblastoma cells did not show firm binding to P-selectin-Fc-fusion protein, but showed loose cell tethering. Similar contradictory results between selectin binding in FACS analyses and under shear stress were found for small cell lung cancer cells and were explained by the binding force hypothesis [26]. This hypothesis would also fit our observation in neuroblastoma cells. It means that P-selectin has several binding partners on the cells, but only a weak binding force resulting in loose tethering of many cells to P-selectin-Fc-fusion protein in the flow assay, while very few E-selectin binding sites induce firm adhesion of only few cells [26].

Adhesive behavior of SK-N-SH cells to E- and P-selectin-Fc-fusion proteins and endothelial cells in vitro indicate that selectins may play a role for SK-N-SH cell adhesion to endothelial cells in vivo. However, further in vivo experimentation within the SK-N-SH xenograft mouse model showed only a slight association between the development of lung metastases and the presentation of E- and P-selectin on endothelial cells. SK-N-SH cells transplanted into scid mice developed more lung metastases

than the same cells transplanted into scid select mice, but the difference did not reach statistical significance in *t* test analysis ($p = 0.052$; Fig. 3: SK-N-SH lung metastases). In ANCOVA analysis, number of lung metastases was compared taking the primary tumor weight into account. In this analysis the number of SK-N-SH lung metastases was significantly higher in scid mice than in scid select mice (factor 6.8, $p < 0.05$; Fig. 3: ANCOVA). However, selectins are obviously not necessary for the formation of SK-N-SH metastases in vivo, because SK-N-SH cells are also able to extravasate and produce distant metastases in absence of P- and E-selectin. If SK-N-SH cells mimic the leukocyte adhesion cascade, the number of leukocytes in the lungs of selectin deficient scid mice should be similar to those of wildtype scid mice as well. Indeed, CD45 immunohistochemical detection of leukocytes in mouse lungs showed no difference between number of leukocytes in scid and scid select mice. Both results suggest that other CAMs of the leukocyte adhesion cascade may compensate for the absence of E- and P-selectin, confirming a functional redundancy of this cascade.

In our study, lung metastasis of LAN 1 cells in vivo is independent of P- and E-selectin deficiency. These cells seem to use alternative molecules for adhesion and extravasation. Adhesion of LAN 1 cells to E- and P-selectin under flow conditions is a rare event, likewise to endothelial cells even after stimulation with TNF-α. Nevertheless, LAN 1 cells produce a considerable number of lung metastases in vivo (mean: scid: 4,135, scid select: 2,770). The arrest of tumor cells in the capillary beds of distant organs is mediated by a combination of mechanical trapping and cancer cell adhesion to specific molecules on the vasculature [7, 44]. Thus, in vivo LAN 1 cells may interact with microvascular endothelium under static conditions by mechanical arrest and subsequent adhesive interactions of tumor cells and endothelial cells which are mediated particularly by ITGs and Ig-like CAMs [44].

Analysis of CTCs in blood of LAN 1 mice exhibited significantly more CTCs in scid select (mean: 64,511 cells/ml) than in scid mice (mean: 43,898 cells/ml; $p < 0.05$). Earlier in vivo findings indicate that the increase of CTCs in the blood of scid select mice compared with wildtype mice is most likely due to the lack of attachment of the tumor cells to the endothelial selectins at the site of the future metastasis [38]. This observation in scid mice reflects the situation in immunocompetent mice, where the absence of E- and P-selectin leads to a considerable leukocytosis in the blood because selectin deficiency hinders the extravasation of leukocytes [41]. However, LAN 1 cells extravasate independent of E- and P-selectin, so that the reasons for this difference of LAN 1 CTCs between scid and scid select mice are unclear so far.

Quantitative real time PCR arrays of CAMs were performed in order to identify CAMs whose expression correlates with the different metastatic pattern of LAN 1 and SK-N-SH cells. In the PCR array CD44, ICAM-1 and ITGA5 and B1 were upregulated, NCAM and VCAM-1 were downregulated in SK-N-SH cells compared with LAN 1 cells.

FACS analysis and previous immunohistochemical studies have already shown that in vitro and in vivo grown LAN 1 cells are CD44 negative, but SK-N-SH cells are CD44 positive [25]. CD44 is implicated in cell–cell and cell–matrix adhesions and is the major cell surface receptor for hyaluronan acid (HA), but has also binding domains for other glycosaminoglycans, collagen, laminin and fibronectin [42, 43]. Furthermore, a specialized sialofucosylated glycoform of CD44 (HCELL, Hematopoietic Cell E/L-selectin Ligand) is a very potent E-selectin ligand [43]. The function of CD44 glycotypes as E-selectin ligand is not relevant in the selectin deficient mice inoculated with SK-N-SH. However, its function as a receptor for HA is still possible. HA is predominatly localized in the periarteriolar space in mouse lungs just as CD44 positive SK-N-SH lung metastases [25, 44]. In vitro SK-N-SH cells adhere to HA, which can be blocked by an anti-CD44 antibody. These results confirm the importance of hyaluronan—CD44 interactions for SK-N-SH cell adhesion and metastasis formation in scid mice.

NCAM is overexpressed in LAN 1, but not in SK-N-SH cells. NCAM is involved in the formation of homotypic tumor cell aggregates, but can also act as a plasticity-promoting molecule by decreasing the overall cell adhesion [45–48]. The key regulator between these two opposite functions of NCAM is polysialic acid, which facilitates the migration of the cells from the primary tumor and is consistently expressed by LAN-1 cells [49–51]. The extraordinary high number of LAN 1 CTCs in blood in both mouse groups (mean: 54,204 cells/ml) in our study indicates that polySia-NCAM positive LAN-1 cells have a great potential to disperse from the primary tumor and to intravasate.

ITGs are transmembrane heterodimers consisting of α and β subunits that bind to CAMs and the extracellular matrix [52]. The function of ITGs is well described in the literature and its relevance in neuroblastoma metastasis is commonly agreed upon [17, 53, 54]. ITGB1 is described as a mediator for cell attachment to extracellular matrix proteins as fibronectin and collagen IV in neuroblastoma [55, 56]. The association of ITGB1 with different α-chains modulates adhesion to and interaction with specific ECM proteins [56]. ITGA5B1 specifically recognizes fibronectin, which is a well-studied matrix glycoprotein [57]. Cell–matrix interactions via ITGs are involved in regulation of cell growth, differentiation, proliferation, adhesion and migration. Recent studies have shown that blocking of ITGA5B1 or ITGB1 is associated with increased

migration, but decreased adhesion to endothelial cells [54, 58]. Our results show that ITGA5 is higher expressed in SK-N-SH than in LAN 1 cells, whereas differences of ITGB1 expression are less pronounced. Silencing of ITGA5 in SK-N-SH cells by RNAi promotes migration significantly. However, SK-N-SH cells showed a higher migratory potential in vitro than LAN 1 cells suggesting that ITGA5 alone did not determine migratory potential of neuroblastoma cells.

Both neuroblastoma cell lines express N-cadherin without differences in staining intensity. Cadherins are calcium dependent, homophilic adhesion molecules. Cadherins are involved in the EMT of epithelial cancer cells and have already been identified as a potential target in the anticancer therapy [59, 60]. Furthermore, N-cadherin has shown to be involved in the rolling of neutrophil granulocytes and breast cancer cells to pulmonary endothelium [61].

Immunohistochemical analyses of N-cadherin and ITGB1 expression showed a stronger staining of the cells grown in culture and the lung metastasis than of the primary tumor. One reason for the different pattern of CAMs of cells grown in culture and primary tumors may be the EMT, which is associated with changes in CAM expression as immotile epithelial cells switch to a cell type with mesenchymal characteristics prior to intravasation into blood vessels. These tumor cells travel as mesenchymal cells through the blood vessels and extravasate into distant sites where they can stay in a mesenchymal appearance or regress to their original epithelial structure [10].

As shown above, the role of individual CAMs expressed in neuroblastoma cells for metastasis formation is complex and various aspects have still to be investigated. Our results indicate a molecular redundancy of tumor cell adhesion and extravasation cascade showing that neuroblastoma cells express several adhesion molecules involved in the leukocyte adhesion cascade varying between the different neuroblastoma cell lines. We can summarize, that selectin-mediated rolling is not required for metastasis formation of LAN 1 and SK-N-SH neuroblastoma cells in vivo. LAN 1 cells extravasate independent of E- and P-selectin and the number of SK-N-SH lung metastases shows only a slight association to endothelial selectin expression. However, CD44, N-cadherin, NCAM and ITGs were upregulated or downregulated, respectively, in SK-N-SH and LAN 1 cells, and can thus be called potential adhesion molecules involved in the metastatic cascade for future studies.

Conflict of interest All authors have no personal or financial conflict of interest and have not entered into any agreement that could interfere with our access to the data on the research, or upon our ability to analyze the data independently, to prepare manuscripts, and to publish them.

References

1. Brodeur GM (2003) Neuroblastoma: biological insights into a clinical enigma. Nat Rev Cancer 3(3):203–216
2. Maris JM, Hogarty MD, Bagatell R et al (2007) Neuroblastoma. Lancet 369(9579):2106–2120
3. Ara T, DeClerck YA (2006) Mechanisms of invasion and metastasis in human neuroblastoma. Cancer Metastasis Rev 25(4):645–657
4. DuBois SG, Kalika Y, Lukens JN et al (1999) Metastatic sites in stage IV and IVS neuroblastoma correlate with age, tumor biology, and survival. J Pediatr Hematol Oncol 21(3):181–189
5. Konstantopoulos K, Thomas SN (2009) Cancer cells in transit: the vascular interactions of tumor cells. Annu Rev Biomed Eng 11:177–202
6. Strell C, Entschladen F (2008) Extravasation of leukocytes in comparison to tumor cells. Cell Commun Signal 6:10
7. Ksiazkiewicz M, Markiewicz A, Zaczek AJ (2012) Epithelial-mesenchymal transition: a hallmark in metastasis formation linking circulating tumor cells and cancer stem cells. Pathobiology 79(4):195–208
8. Chaffer CL, Weinberg RA (2011) A perspective on cancer cell metastasis. Science 331(6024):1559–1564
9. Thiery JP, Acloque H, Huang RY et al (2009) Epithelial-mesenchymal transitions in development and disease. Cell 139(5):871–890
10. Thiery JP (2002) Epithelial-mesenchymal transitions in tumour progression. Nat Rev Cancer 2(6):442–454
11. Kim NH, Kim HS, Li XY et al (2011) A p53/miRNA-34 axis regulates Snail1-dependent cancer cell epithelial-mesenchymal transition. J Cell Biol 195(3):417–433
12. Vitali R, Mancini C, Cesi V et al (2008) Slug (SNAI2) down-regulation by RNA interference facilitates apoptosis and inhibits invasive growth in neuroblastoma preclinical models. Clin Cancer Res 14(14):4622–4630
13. Geng Y, Marshall JR, King MR (2011) Glycomechanics of the metastatic cascade: tumor cell-endothelial cell interactions in the circulation. Ann Biomed Eng 40(4):790–805
14. Pignatelli M, Vessey CJ (1994) Adhesion molecules: novel molecular tools in tumor pathology. Hum Pathol 25(9): 849–856
15. Kim YJ, Borsig L, Varki NM et al (1998) P-selectin deficiency attenuates tumor growth and metastasis. Proc Natl Acad Sci USA 95(16):9325–9330
16. Rosette C, Roth RB, Oeth P et al (2005) Role of ICAM1 in invasion of human breast cancer cells. Carcinogenesis 26(5):943–950
17. Yoon KJ, Danks MK (2009) Cell adhesion molecules as targets for therapy of neuroblastoma. Cancer Biol Ther 8(4):306–311
18. Bendas G, Borsig L (2012) Cancer cell adhesion and metastasis: selectins, integrins, and the inhibitory potential of heparins. Int J Cell Biol 2012:676731
19. Läubli H, Borsig L (2010) Selectins promote tumor metastasis. Semin Cancer Biol 20(3):169–177
20. Witz IP (2008) The selectin–selectin ligand axis in tumor progression. Cancer Metastasis Rev 27(1):19–30
21. Desgrosellier JS, Cheresh DA (2010) Integrins in cancer: biological implications and therapeutic opportunities. Nat Rev Cancer 10(1):9–22

22. Barthel SR, Gavino JD, Descheny L et al (2007) Targeting selectins and selectin ligands in inflammation and cancer. Expert Opin Ther Targets 11(11):1473–1491

23. Stone JP, Wagner DD (1993) P-selectin mediates adhesion of platelets to neuroblastoma and small cell lung cancer. J Clin Invest 92(2):804–813

24. Valentiner U, Haane C, Nehmann N et al (2009) Effects of bortezomib on human neuroblastoma cells in vitro and in a metastatic xenograft model. Anticancer Res 29(4):1219–1225

25. Valentiner U, Valentiner FU, Schumacher U (2008) Expression of CD44 is associated with a metastatic pattern of human neuroblastoma cells in a SCID mouse xenograft model. Tumour Biol 29(3):152–160

26. Richter U, Schroder C, Wicklein D et al (2011) Adhesion of small cell lung cancer cells to E- and P-selectin under physiological flow conditions: implications for metastasis formation. Histochem Cell Biol 135(5):499–512

27. Jojovic M, Schumacher U (2000) Quantitative assessment of spontaneous lung metastases of human HT29 colon cancer cells transplanted into SCID mice. Cancer Lett 152(2):151–156

28. Nehmann N, Wicklein D, Schumacher U et al (2010) Comparison of two techniques for the screening of human tumor cells in mouse blood: quantitative real-time polymerase chain reaction (qRT-PCR) versus laser scanning cytometry (LSC). Acta Histochem 112(5):489–496

29. Schneider T, Osl F, Friess T et al (2002) Quantification of human Alu sequences by real-time PCR–an improved method to measure therapeutic efficacy of anti-metastatic drugs in human xenotransplants. Clin Exp Metastasis 19(7):571–582

30. Remmele W, Stegner HE (1987) Recommendation for uniform definition of an immunoreactive score (IRS) for immunohistochemical estrogen receptor detection (ER-ICA) in breast cancer tissue. Pathologe 8(3):138–140

31. Weber K, Mock U, Petrowitz B (2010) Lentiviral gene ontology (LeGO) vectors equipped with novel drug-selectable fluorescent proteins: new building blocks for cell marking and multi-gene analysis. Gene Ther 17(4):511–520

32. Weber K, Thomaschewski M, Benten D, et al. RGB marking with lentiviral vectors for multicolor clonal cell tracking. Nat Protoc; 7 (5): 839-49

33. Beyer WR, Westphal M, Ostertag W et al (2002) Oncoretrovirus and lentivirus vectors pseudotyped with lymphocytic choriomeningitis virus glycoprotein: generation, concentration, and broad host range. J Virol 76(3):1488–1495

34. Mousa SA (2008) Cell adhesion molecules: potential therapeutic and diagnostic implications. Mol Biotechnol 38(1):33–40

35. Kannagi R, Izawa M, Koike T et al (2004) Carbohydrate-mediated cell adhesion in cancer metastasis and angiogenesis. Cancer Sci 95(5):377–384

36. Läubli H, Borsig L (2009) Heparins attenuate cancer metastasis: are selectins the link? Cancer Invest 27(5):474–481

37. Gebauer F, Wicklein D, Stubke K et al (2013) Selectin binding is essential for peritoneal carcinomatosis in a xenograft model of human pancreatic adenocarcinoma in pfp–/rag2–mice. Gut 62(5):741–750

38. Köhler S, Ullrich S, Richter U et al (2010) E-/P-selectins and colon carcinoma metastasis: first in vivo evidence for their crucial role in a clinically relevant model of spontaneous metastasis formation in the lung. Br J Cancer 102(3):602–609

39. Laferriere J, Houle F, Huot J (2004) Adhesion of HT-29 colon carcinoma cells to endothelial cells requires sequential events involving E-selectin and integrin beta4. Clin Exp Metastasis 21(3):257–264

40. Stübke K, Wicklein D, Herich L et al (2012) Selectin-deficiency reduces the number of spontaneous metastases in a xenograft model of human breast cancer. Cancer Lett 321(1):89–99

41. Frenette PS, Mayadas TN, Rayburn H et al (1996) Susceptibility to infection and altered hematopoiesis in mice deficient in both P- and E-selectins. Cell 84(4):563–574

42. Misra S, Heldin P, Hascall VC et al (2011) Hyaluronan-CD44 interactions as potential targets for cancer therapy. FEBS J 278(9):1429–1443

43. Jacobs PP, Sackstein R (2011) CD44 and HCELL: preventing hematogenous metastasis at step 1. FEBS Lett 585(20):3148–3158

44. Richter U, Wicklein D, Geleff S et al (2012) The interaction between CD44 on tumour cells and hyaluronan under physiologic flow conditions: implications for metastasis formation. Histochem Cell Biol 137(5):687–695

45. Wai Wong C, DE Dye, Coombe (2012) The role of immunoglobulin superfamily cell adhesion molecules in cancer metastasis. Int J Cell Biol 2012:340296

46. Rutishauser U (2008) Polysialic acid in the plasticity of the developing and adult vertebrate nervous system. Nat Rev Neurosci 9(1):26–35

47. Jensen M, Berthold F (2007) Targeting the neural cell adhesion molecule in cancer. Cancer Lett 258(1):9–21

48. Rao Y, Wu XF, Gariepy J et al (1992) Identification of a peptide sequence involved in homophilic binding in the neural cell adhesion molecule NCAM. J Cell Biol 118(4):937–949

49. Hildebrandt H, Mühlenhoff M, Gerardy-Schahn R (2010) Polysialylation of NCAM. Adv Exp Med Biol 663:95–103

50. Yang P, Major D, Rutishauser U (1994) Role of charge and hydration in effects of polysialic acid on molecular interactions on and between cell membranes. J Biol Chem 269(37):23039–23044

51. Valentiner U, Muhlenhoff M, Lehmann U et al (2011) Expression of the neural cell adhesion molecule and polysialic acid in human neuroblastoma cell lines. Int J Oncol 39(2):417–424

52. Brakebusch C, Bouvard D, Stanchi F et al (2002) Integrins in invasive growth. J Clin Invest 109(8):999–1006

53. Favrot MC, Combaret V, Goillot E et al (1991) Expression of integrin receptors on 45 clinical neuroblastoma specimens. Int J Cancer 49(3):347–355

54. Meyer A, van Golen CM, Kim B et al (2004) Integrin expression regulates neuroblastoma attachment and migration. Neoplasia 6(4):332–342

55. Nagae M, Re S, Mihara E et al (2012) Crystal structure of alpha5beta1 integrin ectodomain: atomic details of the fibronectin receptor. J Cell Biol 197(1):131–140

56. Rozzo C, Ratti P, Ponzoni M et al (1993) Modulation of alpha 1 beta 1, alpha 2 beta 1 and alpha 3 beta 1 integrin heterodimers during human neuroblastoma cell differentiation. FEBS Lett 332(3):263–267

57. Labat-Robert J (2002) Fibronectin in malignancy. Semin Cancer Biol 12(3):187–195

58. Scholz M, Blaheta RA, Wittig B et al (2000) Cytomegalovirus-infected neuroblastoma cells exhibit augmented invasiveness mediated by beta1alpha5 integrin (VLA-5). Tissue Antigens 55(5):412–421

59. Blaschuk OW, Devemy E (2009) Cadherins as novel targets for anti-cancer therapy. Eur J Pharmacol 625(1–3):195–198

60. Makrilia N, Kollias A, Manolopoulos L et al (2009) Cell adhesion molecules: role and clinical significance in cancer. Cancer Invest 27(10):1023–1037

61. Strell C, Lang K, Niggemann B et al (2007) Surface molecules regulating rolling and adhesion to endothelium of neutrophil granulocytes and MDA-MB-468 breast carcinoma cells and their interaction. Cell Mol Life Sci 64(24):3306–3316

Darstellung der Publikation

Hintergrund

Das Neuroblastom ist ein embryonaler, hoch maligner Tumor, der aus dem sympathischen Nervensystem abstammt. Es ist der häufigste solide Tumor des Kindesalters und ist beim Zeitpunkt der Diagnose bereits bei 70 % der Kinder in weitere Organe metastasiert. Der Erfolg der Therapie ist beim Vorliegen der Metastasierung sehr gering (1, 2).

Um Ansätze für Therapien zur Behandlung von Neuroblastomen zu identifizieren, ist es notwendig ein tiefgreifendes Verständnis der Vorgänge bei der Metastasierung zu erlangen. Im Rahmen des vorliegenden Projekts wurde die Rolle mehrerer Zelladhäsionsmoleküle (cell adhesion molecules = CAMs) für die Metastasierung humaner Neuroblastomzellen in einem Xenograft Modell untersucht. Zu den Hauptfamilien der CAMs gehören die Selektine, Integrine (ITGs), Cadherin-Superfamilie und Immunglobulin-Superfamilie (ICAM-1, VCAM-1, NCAM) die in entzündlichen Prozessen die Adhäsion der Leukozyten und Thrombozyten zum Endothel vermitteln und in verschiedenen Studien mit der Metastasierung von Tumorzellen in Verbindung gebracht werden (3).

Die Metastasierung von Tumorzellen ist ein sehr komplexer Prozess. Er umfasst die Schritte von der Separation der Tumorzellen aus einem Primärtumor und der lokalen Invasion ins Bindegewebe, über die Einwanderung der Zellen in die Blut- und Lymphgefäße und der Umgehung der Wirtsabwehr während des Aufenthalts im Blutkreislauf, bis zur Adhäsion an das vaskuläre Endothel in entfernten Organen und die Extravasation und Kolonisierung an der Stelle der zukünftigen Metastase (4). Die Rolle der Zelladhäsionsmoleküle während der metastatischen Kaskade ist teilweise gegenläufig reguliert. Einerseits sind epitheliale Zellen unbeweglich und eng an die Basalmembran gebunden, so dass für die Trennung und lokale Invasion von Tumorzellen Zelladhäsionsmoleküle, die Zellkontakte zum Primärtumor vermitteln, herunterreguliert werden müssen. Es wird davon ausgegangen, dass die Migration und Invasion von epithelialen Tumorzellen mit tiefgreifenden phänotypischen Veränderungen einhergehen. Diese beinhalten den Verlust von Zell-Zelladhäsion, den Verlust der Zellpolarität und die Erlangung von migratorischen und invasiven Eigenschaften, die als epithelialer mesenchymaler Übergang (epithelial to mesenchymal transition = EMT) bezeichnet werden (5, 6). Obwohl das Neuroblastom

ein embryonaler Tumor ist und dem sympathischen Nervensystem entspringt, unterliegen die Zellen dem Mechanismus der EMT, wenn sie einen invasiven oder metastatischen Phänotyp eingehen (7, 8). Demgegenüber müssen Zelladhäsionsmoleküle, die die Bindung an Endothelzellen vermitteln, bei der Extravasation hochreguliert werden. Die Interaktionen zwischen zirkulierenden Tumorzellen und Endothelzellen sind als initialer Schritt bei der Bildung einer Metastase notwendig. Diese Interaktionen werden von einer Vielzahl von Zelladhäsionsmolekülen vermittelt, wie zum Beispiel den Selektinen, die auch an der Leukozytenadhäsionskaskade beteiligt sind (3). Folglich basieren jüngste Studien über Tumorzell-Endothelzell Interaktionen auf dem Modell der Leukozyten Extravasation während einer Entzündungsreaktion (9-14). Im Neuroblastom vermittelt P-Selektin die Bindung zwischen Tumorzellen und Thrombozyten, die generelle Bedeutung der Selektine für die Metastasierung von Neuroblastomzellen ist noch nicht bekannt (13, 15, 16).

Das Ziel des dargestellten Projektes ist die Untersuchung der spezifischen Bedeutung ausgewählter Selektine, Integrine (ITGs), Cadherine und Immunglobulin-ähnlicher CAMs (ICAM-1, VCAM-1, NCAM), da diese Tumorzelladhäsion vermitteln können und bereits in klinischen und experimentellen Studien mit malignen Prozessen in Verbindung gebracht wurden. Der Einfluss der oben genannten CAMs auf die Adhäsion und Metastasierung von Neuroblastomzellen wurde in vitro und in einem bereits etablierten Tiermodell mit immundefizienten Mäusen untersucht (17, 18). Für die geplanten Experimente wurden die Neuroblastomzelllinien SK-N-SH und LAN 1 aufgrund ihrer unterschiedlichen Ausprägung von Lungenmetastasen ausgewählt. LAN 1 Zellen produzieren zahlreiche Mikrometastasen im alveoären Interstitium, während SK-N-SH Zellen vorwiegend im intra- und periarteriellen Raum der Lunge mehrzellige Metastasen produzieren (18).

Material und Methoden

Um die Fähigkeit der Neuroblastomzellen zur Bindung an E-und P-Selektin-Fc-Chimäre und die Expression der Selektin Liganden CA19-9 und CD15 s darzustellen, wurde eine Durchflusszytometrie durchgeführt. Dazu wurden die Zellen mit monoklonalen Antikörpern beziehungsweise Selektinkomplexen versetzt und anschließend im FACS-Calibur analysiert. Diese Untersuchung wurde ebenfalls für

die Zelladhäsionsmoleküle CD44, ICAM-1, NCAM, VCAM-1, ITGA5 und ITGB1 durchgeführt.

In Zellflussexperimenten wurde das Bindungsverhalten der Neuroblastomzellen an humanes E- und P-Selektin analysiert. Dazu wurden Objektträger mit rekombinantem humanem (rh) E- beziehungsweise P-Selektin-Fc-Chimären beschichtet und die Adhäsion der Neuroblastomzellen bei unterschiedlich starker Scherkraft untersucht. Als Negativkontrolle wurde rh IgG1-Fc verwendet. Mit dem Versuchsaufbau werden die dynamischen Bedingungen beim Kontakt der Tumorzellen mit Endothelzellen in den Gefäßen simuliert. Außerdem wurde die Haftung an humane Lungenendothelzellen (HPMEC), die mit 10 ng/ml TNF-α über vier Stunden stimuliert wurden, untersucht. Nicht stimulierte Lungenendothelzellen dienten als Negativkontrolle. Stimulierte HPMECs, von denen bekannt ist, dass sie E-Selektin exprimieren, wurden im Vorfeld für 30 Minuten mit einem E-Selektin blockierenden Antikörper inkubiert. In einem weiteren Versuch wurde das Anhaftungsverhalten an eine Hyaluronanbeschichtung (1 mg/ml) mit und ohne Vorbehandlung mit einem CD44 blockierenden Antikörper untersucht. Die Zellbewegungen wurde jeweils mit dem CapImage 8.5 Programm aufgenommen und analysiert.

Für die in vivo Versuche wurden jeweils zehn severe combined immundeficient (scid) Mäuse und zehn E-und P-Selektin Knockout scid Mäuse pro Zelllinie verwendet.

Die Zelllinien LAN 1 und SK-N-SH wurden zwei Wochen vor Versuchsbeginn aufgetaut und unter Standardbedingungen kultiviert. Vor der Injektion der Neuroblastomzellen in die Tiere wurden die Zellen in RPMI Medium1:1 mit Matrigel versetzt. Den Mäusen wurden 200 µl der Zellsuspension subkutan zwischen die Schulterblätter gespritzt, was 1×10^6 Zellen entspricht.

Sobald die Tumoren auf etwa 10% des Körpergewichts der Maus angewachsen waren, wurden die Mäuse aus dem Versuch genommen. Dazu wurden sie mit einer Ketamin/Rompun Narkose in der Dosierung 0,1 ml pro 10 g Körpergewicht anästhesiert. Nachfolgend wurde aus dem Herzen der Mäuse Blut entnommen, bevor sie durch zervikale Dislokation getötet wurden. Abschließend wurden Primärtumor, Lunge und Knochenmark für die folgenden Versuche entnommen.

Von den in Paraffin eingebetteten Primärtumoren sowie den Lungen wurden 4 µm dicke Schnitte angefertigt und im weiteren Verlauf für die Histologie und Immunhistologie verwendet. Um die systematische Erfassung der Lungenmetastasen vorzubereiten, wurden die Schnitte mit Hämatoxylin-Eosin (H.E.) im Färbeautomaten

nach einem Standardprotokoll gefärbt. Jeweils die mittleren 10 Lungenschnitte wurden unter dem Mikroskop bei 100-facher Vergrößerung ausgewertet. Anschließend wurde aus der Gesamtzahl der erfassten Metastasen der Mittelwert über die analysierten Schnitte gebildet und mit der Anzahl aller Lungenschnitte und dem Faktor 0,8 multipliziert, um die Anzahl der Gesamtmetastasen zu berechnen. Dies entspricht dem Verfahren zum Erfassen der Lungenmetastasen nach Jojovic und Schumacher (19). Für die Immunhistochemie wurden verschiedene Antikörper verwendet, die monoklonalen Antikörper N-Cadherin (1:10000), ICAM-1 (1:500), NCAM (1:500), VCAM-1 (1:3000), CD44 (1:5000), ITGA5 (1:250) und ITGB1 (1:50). Um die Färbung zu verifizieren und die Spezifität des Antikörpers zu überprüfen wurde bei jeder Färbung eine Isotypkontrolle mitgeführt. In allen Färbungen war die Isotypkontrolle ohne Reaktion. Die Schnitte wurden mit dem Zeiss Axioplan Mikroskop ausgewertet und fotografiert und die Intensität der Färbungen wurde in einem modifizierten immunreaktiven Score (IRS) evaluiert.

Zum Nachweis von zirkulierenden Tumorzellen im entnommenen Knochenmark und Blut wurden PCR-Arrays mit dem RT² Profiler PCR Arrays durchgeführt. Dafür wurden bereits etablierte Primer, speziell für repetierende, nicht kodierende humane Alu Sequenzen, verwendet (20, 21).

Ergebnisse

In der Durchflusszytometrie konnte bei den SK-N-SH Zellen eine Bindungsaffinität zum P-Selektin-Fc-Fusionsprotein und weniger ausgeprägt zu den anti-CA19-9 und anti-CD15 s Antikörpern nachgewiesen werden. LAN 1 Zellen zeigten eine moderate Bindung zum P-Selektin-Fc-Fusionsprotein. Nur einzelne LAN 1 Zellen waren positiv für CD15 s und CA19-9. Bei beiden Zellreihen wurden sehr wenige Bindungen an E-Selektin-Fc-Fusionsprotein registriert.

Die Ergebnisse der Zellflussversuche zeigten für beide Zelllinien eine Adhäsion an das E-Selektin-Fc-Fusionsprotein. Für SK-N-SH Zellen wurden speziell bei einer Beschichtung mit 50 µg/ml und einer Scherkraft von 0,5 dyn/cm^2 mehr Bindungsereignisse gemessen als bei LAN 1 Zellen (16 vs. 4 Ereignisse, p < 0.05). Bemerkenswert ist, dass einmal eingegangene Bindungen sich auch unter starken Scherkräften nicht mehr lösten.

Deutlich anders verhielten sich die Tumorzellen auf rh P-Selektin-Fc-Fusionsprotein beschichteten Objektträgern (50 µg/ml). Bei beiden Zelllinien wurden bei 0,5 dyn/cm^2

Scherkraft kaum Zelladhäsionen, sondern stattdessen Tethering nachgewiesen. Bei stärkeren Scherkräften zeigte sich weder Adhäsion noch Tethering von Neuroblastomzellen an P-Selektin-Fc-Fusionsprotein.

Die Untersuchung des Bindungsverhaltens von SK-N-SH Zellen an stimulierte vs. nicht stimulierte HPMECs zeigte stärkeres Bindungsverhalten zu TNF-α stimulierten HPMECs (17 vs. 3 Bindungsgeschehnisse, $p<0.01$).

Nach Behandlung der Objektträger mit dem bindungsblockierendem anti-E-Selektin (CD62E) Antikörper verminderte sich die SK-N-SH Zellbindung um 50% ($p<0.05$). Die Bindung der LAN 1 Zellen zu nicht stimulierten und stimulierten HPMECs unter Scherkräften war nicht nachweisbar bzw. äußerst gering.

Während CD44 negative LAN 1 Zellen nicht an Hyaluronan beschichtete Kapillaren banden, wurden bei CD44 positiven SK-N-SH Zellen 20 Bindungsereignisse dokumentiert. Die Bindung von SK-N-SH Zellen an Hyaluronan wurde vom anti-CD44 Antikörper wirksam blockiert ($p<0.01$).

Im den Tierversuchen entwickelten alle Mäuse Primärtumoren. Das Gewicht der Tumoren unterschied sich nicht signifikant zwischen den scid und scid select Mäusen. Das mittlere Tumorgewicht in der SK-N-SH Gruppe lag bei 1.18 g für beide Mausgruppen. Alle SK-N-SH scid Mäuse und sieben von zehn scid select Mäusen entwickelten Lungenmetastasen. Die Lungenmetastasen der mit SK-N-SH Zellen beimpften Mäuse waren hauptsächlich im intra-und periarteriellen Raum der Lunge lokalisiert und die Bandbreite der Lungenmetastasen der scid Mäuse lag zwischen 144 und 1795 (Mittelwert: 546), die der scid select Mäuse von 0 bis 1240 (Mittelwert: 335). In den scid wildtyp Mäusen, die mit SK-N-SH Zellen beimpft waren, war die Anzahl der Lungenmetastasen um den Faktor 7.2 höher als bei den scid select Mäusen ($p=0.052$). Unter Berücksichtigung des Tumorgewichts als Covariante (ANCOVA), war die Anzahl der SK-N-SH Lungenmetastasen in scid Mäusen um einen Faktor 6.8 signifikant höher als in den scid select Mäusen ($p<0.05$). Die Anzahl der zirkulierenden Tumorzellen in Blut und Knochenmark zeigte keinen signifikanten Unterschied zwischen den scid- und scid-select Mäusen der SK-N-SH Gruppe.

In der LAN 1 Gruppe lag das durchschnittliche Tumorgewicht bei 1.98 g für die scid Mäuse und 2.06 g für die scid select Mäuse. Sieben von zehn scid Mäusen und alle zehn scid select Mäuse, die mit LAN 1 Zellen beimpft waren, entwickelten Lungenmetastasen, die hauptsächlich als Mikrometastasen in den alveolären Septen

auftraten. Die Anzahl der Metastasen schwankte zwischen 0 und 11543 (Mittelwert: 4135) in den scid Mäusen und zwischen 594 und 8624 (Mittelwert: 2770) in den scid select Mäusen. Statistisch ließ sich kein signifikanter Zusammenhang zwischen der Anzahl der Metastasen in den scid und scid select Mäusen erkennen. Die Anzahl der LAN 1 zirkulierenden Tumorzellen im Blut war in den scid select Mäusen um den Faktor 7.0 höher als in den scid Mäusen ($p<0.05$). Der Mittelwert von zirkulierenden Tumorzellen im Knochenmark lag bei den scid Mäusen bei 189 Zellen/ml und bei den scid select Mäusen bei 417 Zellen/ml Knochenmark. Die Experimente ergaben eine Erhöhung der Anzahl um den Faktor 3.9 bei den scid select Mäusen gegenüber den scid Mäusen ($p<0.01$). Vergleicht man die LAN 1 und SK-N-SH scid Mäuse, so war die Anzahl der zirkulierenden Tumorzellen im Blut und der Lungenmetastasen signifikant niedriger in den SK-N-SH scid Mäusen als in den LAN 1 scid Mäusen ($p<0.001$ und $p<0.01$).

Die Messung von mRNA mittels Echtzeit PCR zeigte eine höhere Expression von ITGA5 ($p<0.05$), ITGB1 ($p<0.05$), ICAM-1 ($p<0.05$) und CD44 (nicht signifikant) mRNA in SK-N-SH Zellen im Vergleich zu den LAN 1 Zellen. Jedoch war in den LAN 1 Zellen die mRNA von NCAM 1 ($p<0.05$) und VCAM-1 (nicht signifikant) höher reguliert als in SK-N-SH Zellen.

Die immunhistologischen Färbungen der Primärtumoren und Lungen zeigten keine Unterschiede in den scid und scid select Mäusen innerhalb einer Gruppe und korrespondierten überwiegend mit den Ergebnissen der Durchflusszytometrie.

Zusammenfassend lässt sich darstellen, dass in der Immunhistochemie die SK-N-SH Zellen CD44, ITGA5 und B1 ausgeprägter exprimieren als die LAN 1 Zellen. Jedoch waren SK-N-SH Zellen negativ für NCAM, welches wiederum stark von den LAN 1 Zellen exprimiert wurde. Die anti-N-Cadherin Immunhistochemie zeigte bei beiden Neuroblastomzelllinien eine starke Färbung. ICAM-1 und VCAM-1 konnte in der Immunhistochemie in keiner der Zelllinien nachgewiesen werden. Die Färbeintensität mit anti-N-Cadherin und anti-ITGB1 war für beide Zelllinien schwächer in den Primärtumoren als in den in vitro gewachsenen Zellen und Lungenmetastasen.

Diskussion

Die Ergebnisse unserer in vitro Versuche legen nahe, dass Selektine je nach Zelllinie einen unterschiedlich starken Einfluss auf die Adhäsion von Neuroblastomzellen aufweisen. Im Zellflussversuch gingen die LAN 1 Zellen lediglich schwache Bindungen an das rekombinante E-Selektin-Fc-Fusionsprotein (4 Ereignisse) und an durch TNF-α stimulierte HPMECs (3 Ereignisse) ein. SK-N-SH Zellen hingegen zeigten mehr Bindungsereignisse zum rekombinanten E-Selektin-Fc-Fusionsprotein (16 Ereignisse) und den stimulierten HPMECs (17 Ereignisse). Die Bindung von SK-N-SH Zellen zu stimulierten HPMECs wurde durch einen anti-E-Selektin-Antikörper wirksam reduziert (8 Ereignisse). Das deutet auf eine Interaktion dieser Zellen mit E-Selektin hin. Unter Flussbedingungen zeigten beide Zelllinien Tethering, aber keine stabile Adhäsion an rekombinantes P-Selektin-Fc-Fusionsprotein. In der Durchflusszytometrie wurden die E-Selektin Liganden CA19-9 und CD15 s nur von wenigen Zellen der beiden Zellreihen exprimiert. SK-N-SH und LAN 1 Zellen gingen mit dem E-Selektin-Fc-Fusionsprotein nur eine schwache Bindung ein. Im Gegensatz dazu zeigten beide eine moderate Bindung an das P-Selektin-Fc-Fusionsprotein, was im Widerspruch zu den Ergebnissen der Zellflussversuche steht. Für kleinzellige Bronchialkarzinomzellen wurden ähnliche Ergebnisse beschrieben, die auf die unterschiedlichen Bindungskräfte der Zellen zu E- bzw. P-Selektin unter dynamischen Bedingungen (Bindung, Rollen, Tethering) zurückgeführt wurden (22).

Unsere in vivo Versuche ergaben, dass LAN 1 Zellen genau wie die SK-N-SH Zellen auch in Abwesenheit von E-und P-Selektin Lungenmetastasen ausbilden. Die Zellen scheinen alternative Moleküle zur Zellbindung und Extravasation zu nutzen. Die Analyse der zirkulierenden Tumorzellen im Blut von LAN 1 Mäusen ergab eine signifikant erhöhte Anzahl von Tumorzellen in dem Blut der scid select Mäuse. Frühere in vivo Versuche mit anderen Tumorzellen führen dies auf einen Mangel von Befestigungsmechanismen der Tumorzelle an die Selektine der Endothelzellen der zukünftigen Metastase zurück (23). Diese Beobachtungen in den scid Mäusen entsprechen dem Verhalten immunkompetenter Mäuse, bei denen die Abwesenheit von E-und P-Selektin zu einer beträchtlichen Leukozytose im Blut führt, da das Fehlen der Selektine die Extravasation der Leukozyten behindert (24). Dies erklärt allerdings nicht die erhöhte Anzahl der zirkulierenden LAN 1 Tumorzellen im Blut in

selektindefizienten Mäusen, da diese Zellen unabhängig von E-und P-Selektin zur Extravasation in der Lage sind.

Um Zelladhäsionmoleküle zu identifizieren, die unterschiedlich in LAN 1 und SK-N-SH Zellen exprimiert werden, wurden Polymerasekettenreaktionen durchgeführt, die ergaben, dass CD44, ICAM-1, ITGA5 und B1 in SK-N-SH Zellen hochreguliert waren. NCAM und VCAM-1 waren in den SK-N-SH Zellen runterreguliert. Durchflusszytometrische und immunhistologische Untersuchungen haben in vitro und in vivo gezeigt, dass LAN 1 Zellen negativ für CD44 sind, während SK-N-SH positiv sind (18). Da SK-N-SH Zellen auch in den selektindefizienten Mäusen Metastasen entwickeln, scheint hier die Rolle von CD44 als E-Selektin-Ligand nicht entscheidend zu sein. Weitere Versuche sollten klären, ob CD44 eine Rezeptorfunktion für Hyaluronsäure erfüllt, da diese ebenso wie die CD44 positiven SK-N-SH Lungenmetastasen vorwiegend im periarteriellen Raum der Mauslungen lokalisiert sind (18, 25). In vitro binden die SK-N-SH Zellen an Hyaluronsäure. Dass die Bindungen durch anti-CD44-Antikörper geblockt werden können, stützt die Annahme der Interaktionen von Hyaluronsäure und CD44 bei der SK-N-SH Zelladhäsion und deren Mitwirkung bei der Metastasenbildung in scid Mäusen.

Unsere Ergebnisse zeigen, dass ITGA5 in SK-N-SH Zellen stärker exprimiert ist, als in LAN 1 Zellen. In der Expression von ITGB1 sind weniger Unterschiede zwischen den Zelllinien zu finden. SK-N-SH Zellen zeigten in vitro ein höheres Migrationspotenzial als LAN 1 Zellen. Ein knockdown von ITGA5 mittels shRNA erhöhte allerdings das Migrationspotenzial der SK-N-SH Zellen was darauf hindeutet, dass ITGA5 nicht allein die Migration der Zellen bestimmt.

Beide Neuroblastomzellreihen exprimierten N-Cadherin ohne Unterschiede in der Färbeintensität. N-Cadherin wird mit dem Zellrollen von neutrophilen Granulozyten und Brustkrebszellen zum Lungenendothel in Verbindung gebracht und ist bereits als potenzieller Angriffspunkt bei der Krebstherapie identifiziert (26 -28).

Immunhistochemische Analysen von N-Cadherin und ITGB1 zeigten intensivere Färbeergebnisse bei den Zellen, die in Kultur gewachsen waren und den Lungenmetastasen, als bei den Primärtumoren. Ein Grund für das unterschiedliche Expressionsmuster der CAMs der Zellen in Kultur und der Primärtumoren kann die EMT sein, die ebenfalls mit Veränderungen der CAM Expression assoziiert ist. Unbewegliche Epithelzellen wandeln sich zu Zelltypen mit mesenchymalem Charakter, bevor sie in die Blutgefäße einwandern. Diese Tumorzellen wandern als

mesenchymale Zellen durch die Blutgefäße in entfernte Organe, wo sie entweder als mesenchymale Zellen bleiben oder sich in ihre epitheliale Form zurückbilden (29).

Wie oben beschrieben ist die Rolle der verschiedenen Zelladhäsionsmoleküle in Neuroblastomzellen in Bezug auf die Metastasierung sehr komplex und verschiedene Aspekte müssen noch genauer untersucht werden. Da die Neuroblastomzellen verschiedene Zelladhäsionsmoleküle exprimieren, die in die Leukozytenadhäsion einbezogen sind und sich auch zwischen den zwei Zelllinien unterscheiden, lassen unsere Ergebnisse eine molekulare Redundanz in der Kaskade von Tumorzelladhäsion und Extravasation vermuten. Man kann zusammenfassen, dass Selektin vermitteltes Zellrollen nicht notwendig für den Metastasierungsprozess von LAN 1 und SK-N-SH Zellen in vivo ist. LAN 1 Zellen können unabhängig von E-bzw. P-Selektin aus den Gefäßen auswandern, und die Anzahl der Lungenmetastasen der SK-N-SH Zellen zeigen nur eine geringfügige Assoziation zur Selektinexpression auf den Endothelzellen. Es bestehen jedoch Unterschiede bezüglich der Expression von CD44, N-Cadherin, NCAM und ITGs zwischen den beiden Zelllinien, deren Einfluss auf den Metastasierungsprozess von Neuroblastomzellen in zukünftigen Studien untersucht werden soll.

Quellen

1. Brodeur GM (2003) Neuroblastoma: biological insights into a clinical enigma. Nat Rev Cancer 3(3):203–216

2. Maris JM, Hogarty MD, Bagatell R et al (2007) Neuroblastoma. Lancet 369(9579):2106–2120

3. Geng Y, Marshall JR, King MR (2011) Glycomechanics of the metastatic cascade: tumor cell-endothelial cell interactions in the circulation. Ann Biomed Eng 40(4):790–805

4. Konstantopoulos K, Thomas SN (2009) Cancer cells in transit: the vascular interactions of tumor cells. Annu Rev Biomed Eng 11:177–202

5. Ksiazkiewicz M, Markiewicz A, Zaczek AJ (2012) Epithelial- mesenchymal transition: a hallmark in metastasis formation linking circulating tumor cells and cancer stem cells. Pathobiol- ogy 79(4):195–208

6. Chaffer CL, Weinberg RA (2011) A perspective on cancer cell metastasis. Science 331(6024):1559–1564

7. Kim NH, Kim HS, Li XY et al (2011) A p53/miRNA-34 axis regulates Snail1-dependent cancer cell epithelial-mesenchymal transition. J Cell Biol 195(3):417–433

8. Vitali R, Mancini C, Cesi V et al (2008) Slug (SNAI2) down- regulation by RNA interference facilitates apoptosis and inhibits invasive growth in neuroblastoma preclinical models. Clin Can- cer Res 14(14):4622–4630

9. Strell C, Entschladen F (2008) Extravasation of leukocytes in comparison to tumor cells. Cell Commun Signal 6:10

10. Pignatelli M, Vessey CJ (1994) Adhesion molecules: novel molecular tools in tumor pathology. Hum Pathol 25(9): 849–856

11. Kim YJ, Borsig L, Varki NM et al (1998) P-selectin deficiency attenuates tumor growth and metastasis. Proc Natl Acad Sci USA 95(16):9325–9330

12. Rosette C, Roth RB, Oeth P et al (2005) Role of ICAM1 in invasion of human breast cancer cells. Carcinogenesis 26(5):943–950

13. Yoon KJ, Danks MK (2009) Cell adhesion molecules as targets for therapy of neuroblastoma. Cancer Biol Ther 8(4):306–311

14. Bendas G, Borsig L (2012) Cancer cell adhesion and metastasis: selectins, integrins, and the inhibitory potential of heparins. Int J Cell Biol 2012:676731

15. Barthel SR, Gavino JD, Descheny L et al (2007) Targeting selectins and selectin ligands in inflammation and cancer. Expert Opin Ther Targets 11(11):1473–1491

16. Stone JP, Wagner DD (1993) P-selectin mediates adhesion of platelets to neuroblastoma and small cell lung cancer. J Clin Invest 92(2):804–813

17. Valentiner U, Haane C, Nehmann N et al (2009) Effects of bortezomib on human neuroblastoma cells in vitro and in a metastatic xenograft model. Anticancer Res 29(4):1219–1225

18. Valentiner U, Valentiner FU, Schumacher U (2008) Expression of CD44 is associated with a metastatic pattern of human neu- roblastoma cells in a SCID mouse xenograft model. Tumour Biol 29(3):152–160

19. Jojovic M, Schumacher U (2000) Quantitative assessment of spontaneous lung metastases of human HT29 colon cancer cells transplanted into SCID mice. Cancer Lett 152(2):151–156

20. Nehmann N, Wicklein D, Schumacher U et al (2010) Comparison of two techniques for the screening of human tumor cells in mouse blood: quantitative real-time polymerase chain reaction (qRT-PCR) versus laser scanning cytometry (LSC). Acta Histo- chem 112(5):489–496

21. Schneider T, Osl F, Friess T et al (2002) Quantification of human Alu sequences by real-time PCR–an improved method to measure therapeutic efficacy of anti-metastatic drugs in human xeno- transplants. Clin Exp Metastasis 19(7):571–582

22. Richter U, Schroder C, Wicklein D et al (2011) Adhesion of small cell lung cancer cells to E- and P-selectin under physio- logical flow conditions: implications for metastasis formation. Histochem Cell Biol 135(5):499–512

23. Köhler S, Ullrich S, Richter U et al (2010) E-/P-selectins and colon carcinoma metastasis: first in vivo evidence for their crucial role in a clinically relevant model of sponta- neous metastasis formation in the lung. Br J Cancer 102(3):602–609

24. Frenette PS, Mayadas TN, Rayburn H et al (1996) Susceptibility to infection and altered hematopoiesis in mice deficient in both P- and E-selectins. Cell 84(4):563–574

25. Richter U, Wicklein D, Geleff S et al (2012) The interaction between CD44 on tumour cells and hyaluronan under physiologic flow conditions: implications for metastasis formation. Histochem Cell Biol 137(5):687–695

26. Strell C, Lang K, Niggemann B et al (2007) Surface molecules regulating rolling and adhesion to endothelium of neutrophil granulocytes and MDA-MB-468 breast carcinoma cells and their interaction. Cell Mol Life Sci 64(24):3306–3316

26. Blaschuk OW, Devemy E (2009) Cadherins as novel targets for anti-cancer therapy. Eur J Pharmacol 625(1–3):195–198

28. Makrilia N, Kollias A, Manolopoulos L et al (2009) Cell adhesion molecules: role and clinical significance in cancer. Cancer Invest 27(10):1023–1037

29. Thiery JP (2002) Epithelial-mesenchymal transitions in tumour progression. Nat Rev Cancer 2(6):442–454

10. Erklärung des Eigenanteils an der Publikation

Ich erkläre hiermit, dass mein Eigenanteil an der vorliegenden Publikation aus Folgendem bestand:

Durchführung der Experimente unter Aufsicht und Anleitung von Frau Dr. med. Ursula Valentiner, Schreiben der Publikation gemeinsam mit Frau Dr. med. Ursula Valentiner; Verfassen der „Darstellung der Publikation im breiteren Kontext und Erläuterung weiterführender Ergebnisse über die Publikation hinaus"

Danksagung

An erster Stelle möchte ich mich herzlich bei Herrn Prof. Dr. med. Udo Schumacher für die Überlassung des wissenschaftlichen Themas bedanken. Seine stets zuversichtliche Einstellung und freundliche Unterstützung haben sehr dazu beigetragen, mit Freude die Arbeit zu vollenden.

Mein Dank gilt außerdem meiner Betreuerin Frau Dr. med. Ursula Valentiner, die jederzeit für mich als Ansprechpartnerin da war und mir den Einstieg in die Laborarbeit sehr erleichtert hat. Ihre Unterstützung zum selbstständigen Arbeiten hat maßgeblich zu meiner Motivation beigetragen.

Allen Mitarbeitern des Laborteams danke ich für das freundschaftliche Arbeitsklima und die stete Hilfe bei den verschiedenen Experimenten.

Lebenslauf:

Persönliche Daten:

Name: Nina Johanna Schwankhaus-Bade

Geburt: am 24.02.1982 in Kronberg im Taunus

Familienstand: verheiratet

Schulausbildung:

1992 – 2002 Gymnasium Hochrad

Juli 2002 Abitur

Studium:

September 2007 Beginn des Medizinstudiums am Universitätsklinikum Eppendorf in Hamburg

März 2010 Erster Abschnitt der ärztlichen Prüfung

September 2010 Beginn der Doktorarbeit bei Herrn Prof. Dr. med. Udo Schumacher am Institut für Anatomie und experimentelle Morphologie

2013-2014 Praktisches Jahr Innere Medizin in der Asklepios Klinik Sankt Georg, Hamburg

Neurologie in der Asklepios Klinik Sankt Georg, Hamburg

Chirurgie in der Asklepios Klinik Altona, Hamburg

Mai 2014 Zweiter Abschnitt der ärztlichen Prüfung

11. Eidesstattliche Versicherung

Ich versichere ausdrücklich, dass ich die Arbeit selbständig und ohne fremde Hilfe verfasst, andere als die von mir angegebenen Quellen und Hilfsmittel nicht benutzt und die aus den benutzten Werken wörtlich oder inhaltlich entnommenen Stellen einzeln nach Ausgabe (Auflage und Jahr des Erscheinens), Band und Seite des benutzten Werkes kenntlich gemacht habe.

Ferner versichere ich, dass ich die Dissertation bisher nicht einem Fachvertreter an einer anderen Hochschule zur Überprüfung vorgelegt oder mich anderweitig um Zulassung zur Promotion beworben habe.

Ich erkläre mich einverstanden, dass meine Dissertation vom Dekanat der Medizinischen Fakultät mit einer gängigen Software zur Erkennung von Plagiaten überprüft werden kann.

Unterschrift: ....